January 2015

Reliable Power System Planning and Operations through Robust Optimization

Wei Yuan
University of South Florida, will.w.yuan@gmail.com

Reliable Power System Planning and Operations through Robust Optimization

by

Wei Yuan

A dissertation submitted in partial fulfillment
of the requirements for the degree of
Doctor of Philosophy in Industrial Engineering
Department of Industrial and Management Systems Engineering
College of Engineering
University of South Florida

Major Professor: Bo Zeng, Ph.D.
Tapas Das, Ph.D.
Alex Savachkin, Ph.D.
Yao Liu, Ph.D.
Balaji Padmanabhan, Ph.D.
Tongxin Zheng, Ph.D.

Date of Approval:
June 30, 2015

Keywords: Mixed Integer Programming, Network Topology Control, Robust Optimization,
Defender-attacker-defender Model, Distribution Network Planning

DEDICATION

To my loving parents for their endless love, devotion and support.

ACKNOWLEDGMENT

First, I dedicate this dissertation work to my family. I would like to dedicate this work to my parents for their support and help in the past many years.

Second, I would like to dedicate this dissertation to my major advisor, Dr. Bo Zeng, who have been my mentor since 2010. This work cannot be done without his help and support. Sometimes we agreed, and sometimes we argued. Sometimes we succeeded, and sometimes we failed. I am very happy that I have the opportunity to spend fives years working with him at University of South Florida.

Thirdly, I would dedicate this work to Dr. Tapas Das, Dr. Alex Savachkin, Dr. Balaji Padmanabhan, Dr. Yao Liu, and Dr. Tongxin Zheng for serving in my committee and giving me valuable suggestions on my work.

Finally, I would like to thank Dr. Jinye Zhao, Dr. Tongxin Zheng, and Dr. Eugene Litvinov from ISO-New England for their support and constructive advice on my work on robust unit commitment Problem. I would like to thank Dr. Jianhui Wang, Dr. Feng Qiu, and Dr. Chen Chen from Energy System Division, Argonne National Laboratory for their help and directions on the distribution network planning problem.

Lastly, I offer my regards to all of those who supported me in any respect during the completion of this work.

TABLE OF CONTENTS

LIST OF TABLES

LIST OF FIGURES

ABSTRACT

In this dissertation, we introduce and study robust optimization models and decomposition algorithms in order to deal with the uncertainties such as terrorist attacks, natural disasters, and uncertain demand that are becoming more and more significant in power systems operation and planning. An optimal power grid hardening problem is presented as a defender-attacker-defender (DAD) sequential game and solved by an exact decomposition algorithm. Network topology control, which is an effective corrective measure in power systems, is then incorporated into the defender-attacker-defender model as a recourse operation for the power system operator after a terrorist attack. Computational results validate the cost-effectiveness of the novel model. In addition, a resilient distribution network planning problem (RDNP) is proposed in order to coordinate the hardening and distributed generation resource placement with the objective of minimizing the distribution system damage under uncertain natural disaster events. A multi-stage and multi-zone based uncertainty set is designed to capture the spatial and temporal dynamics of a natural disaster as an extension to the N-K worst-case network interdiction approach. Finally, a power market day-ahead generation scheduling problem, i.e., robust unit commitment (RUC) problem, that takes account of uncertain demand is analyzed. Improvements have been made in achieving a fast solution algorithm for the RUC model.

CHAPTER 1: INTRODUCTION

The electric power grid is the largest machine in the whole world. As one of the thirteen critical infrastructures, the power grid is the backbone of our society since almost every aspect of the society relies on the electric power from the power grid. However, the operation and planning models in power systems are getting more and more complicated. The uncertainties that come from terrorist attacks and natural disasters have caused concerns on the vulnerability of the power grids both in the transmission network level and the distribution network level. Moreover, on the one hand, new technologies, such as renewable generation, demand side management, distributed generation, smart grids, etc., have greatly improved the efficiency and reliability of the modern grid. On the other hand, these technologies are adding new complexities such as uncertain renewable generation and demand to the operation models and causing new reliability issues in the power grid. Hence, in order to deal with the more and more significant uncertainties in the power girds, we propose robust optimization based operation and planning models and design decomposition algorithms to solve these models.

In Chapter 2, a power grid protection planning problem on the transmission systems is considered to address the vulnerability issue of uncertain terrorist attacks on the transmission network. The power grid protection problem is often formulated as a tri-level defender-attacker-defender model. However, this tri-level problem is computationally challenging

and no exact solution is provided in the literature. In order to tackle this fundamental problem, in this chapter, we design and implement a decomposition algorithm to derive its optimal solutions. Numerical results are given on an IEEE one-area RTS- 1996 system show that the developed algorithm identifies optimal solutions in a reasonable time, which significantly outperforms an existing algorithm. We also confirm that the protection plan obtained through solving the attacker-defender model does not lead to the optimal protection plan in general.

In Chapter 3, the transmission network topology through transmission line switching, as an effective corrective operation for power system operators to improve the economic operations of the electric transmission network, is modeled and analyzed in the power grid defender-attacker-attacker model framework. The preventive approach, i.e., protection, and the corrective approach, i.e., network topology control, are coordinated in the proposed defender-attacker-defender model with transmission line switching (DAD-TLS). We customize and implement nested decomposition algorithm to derive optimal solutions. Numerical experiments are performed on the IEEE one-area RTS-1996 system. Results verify the benefits of incorporating transmission line switching as a post-contingency operation into DAD model.

Natural disasters such as Hurricane Sandy can seriously disrupt the power grids. To increase the resilience of a distribution system against uncertain natural disasters, Chapter 4 proposes a resilient distribution network planning problem (RDNP) in order to coordinate the hardening and distributed generation resources with the objective of minimizing the

system damage. The problem is formulated as a two-stage robust optimization model. A multi-stage and multi-zone based uncertainty set is designed to capture the spatial and temporal dynamics of an uncertain natural disaster as an extension to the N-K worst-case network interdiction approach. The optimal solution yields a resilient distribution system against natural disasters. A decomposition algorithm is designed to solve this tri-level program. Computational studies demonstrate the effectiveness of the proposed model. The computational results also reveal that distributed generation is important in increasing the resilience of a distribution system against natural disasters in the form of microgrids.

Finally, in Chapter 5, we explore the robust unit commitment (RUC) problem that is considered to be the cornerstone in power systems operations. The two-stage robust unit commitment problem is proposed to deal with various complicated uncertainties in power systems, including those in renewable generation, load realization, demand response, and contingencies. However, such tri-level optimization problem is very challenging to solve, considering large-scale real power grids. In this Chapter, we study new computational methods and strategies to address this challenge, including incorporating strong formulations for basic unit commitment model, deriving new valid inequalities considering network constraints, and designing and implementing a decomposition procedure. On large-scale test instances, our solution approach leads to significantly better computational performance, compared to existing formulations or methods.

This dissertation is organized as follows. Chapter 2 describes the work in designing exact solution power grid defender-attack-defender. Chapter 3 presents a defender-attacker-

defender model with transmission network topology control. Chapter 4 corresponds to a distribution network planning problem against uncertain natural disasters. Chapter 5 presents the work in developing a fast algorithm for robust unit commitment problem.

CHAPTER 2: DEFENDER-ATTACKER-DEFENDER MODEL FOR POWER GRID PROTECTION

2.1 Note to Reader

This chapter has been previously published on Elsevier as: Wei Yuan, Long Zhao and Bo Zeng, optimal power grid protection through a defender-attacker-defender model, Reliability Engineering & System Safety [1]. The second author, Dr. Long Zhao, contributed for part of the technical section. Third author, Dr. Bo Zeng, contributed for identifying the background of this application.

2.2 Background

Power grid vulnerability is a critical issue in modern society. According to a recent study by the National Research Council, a terrorist attack on the U.S. power grid could be much more destructive than natural disasters such as Hurricane Sandy, by blacking out large segments of the country for weeks or even months, costing hundreds of billions of economic damage, and leading to thousands of deaths due to heat stress or exposure to cold during the blackout [2]. Roughly, 200 terrorist attacks on power grids have been reported outside of the U.S. over the past few decades. In fact, from 1999 to 2002, there were over 150 attacks on electric power systems across the world [3]. N-1 and N-2 security criteria [4] are employed by North American Electric Reliability Corporation (NERC) to ensure the normal operations of power grids under one or two disruptions. Unfortunately, power grids are exposed to both

unintentional random failures and terrorist attacks [5]. Hence, simultaneous out-of-service components in a system are not limited to 2. Consequently, N-1 and N-2 criteria are not sufficient to guarantee the security of a power grid under multiple contingencies [4, 6].

Power grid interdiction problem is introduced to identify the set of contingencies that make a power grid most vulnerable. Salmeron et al. [7] formulate a power grid interdiction problem as a max-min bi-level program, or an attacker-defender (AD) game theoretical model, and solve the problem by global Benders decomposition algorithm [8]. It is noted that the system performance under the worst N-1 or N-2 scenarios can be computed through limiting the number of transmission lines under attack to be one or two. Hence, this attacker-defender model provides a framework to perform analysis with the general N-k criterion. Motto et al. [9] transform the bi-level program to an equivalent single-level mixed integer program through dualizing the lower level liner programming problem, and solve the mixed-integer program using available solvers. Zhao and Zeng [10] exactly solve an attacker-defender model with transmission line switching as a mitigation operation. In these models, two different agents, an attacker and a defender optimize their respective objective functions. The attacker, which is the leader in this game and could be a group of terrorists or a natural disaster, seeks to maximize the power grid disruption (penalty in terms of unmet demand or load shed [11]) given limited attacking resources. The defender, i.e., the power grid operator who acts as the follower, reacts after the attack with the goal of minimizing the power grid disruption by re-dispatch. However, even though attacker-defender models are useful in obtaining a set of most critical components for a power grid, protecting those

critical components does not necessarily provide the best protection plan against system disruptions as discussed in [11, 12].

In order to determine an optimal power grid protection plan, Brown et al. [13] propose to extend the bi-level attacker-defender model to a tri-level defender-attacker-defender (DAD) model. As presented in [12–15], a defender-attacker-defender game theoretical model involves three agents acting sequentially: (*i*) the defender's protection: the system planner or defender identifies power system components to be protected or hardened; (*ii*) the attacker's disruption: an attacker disrupts the power grid by forcing the critical system components out of service; and (*iii*) the system operator's mitigation: the operator reacts to the disruptive actions to minimize overall damage by manipulating the power grid components. Both Brown et al. [11] and Yao et al. [12] argue that a tri-level defender-attacker-defender model produces a superior protection plan because it considers an additional level of interaction between the defender and the attacker, and selects the best strategy overall. In fact, the cost of protection plan from an attacker-defender model is 28 percent higher than that of the optimal protection plan from a defender-attacker-defender model for a particular power grid instance in [11]. By introducing an extra level of defender to the model, a defender-attacker-defender model allows the defender to evaluate the impact of varying the defensive resources budget by doing sensitivity analysis that could not be completed by an attacker-defender model alone [12].

Brown et al. [11] initially formulate the optimal allocation of defensive resources problem in a power grid as a defender-attacker-defender model to determine the most critical

network components to be protected against terrorist attacks. Results on some particular instances show that adopting a protection plan based on the optimal interdiction solution from an attacker-defender model would result in a substantial misuse of defensive resources [11]. Yao et al. [12] study a similar tri-level optimization model and describe a decomposition approach that solves smaller bi-level problems iteratively. This approach is actually an extension of set covering decomposition discussed by Israreli and Wood [16]. It is observed from a set of numerical studies that the method in [12] is time-consuming. Delgadillo et al. [15] develop an improved algorithm, the implicit enumeration algorithm, which is within a branch and bound framework, to solve this tri-level programming problem. Their implicit enumeration algorithm is computationally more efficient than the method developed in [12]. However, it may not be efficient to deal with instances with multiple attacks and protection decisions. To reduce the computational burden for this type of problems, Bier et al. [14] propose a simple and inexpensive algorithm that iteratively applies Max Line interdiction algorithm to sequentially identify a promising hardening or interdiction operation. Although this approach determines suboptimal solutions, the computational difficulty is reduced remarkably.

To analytically solve this challenging power grid defender-attacker-defender model, it is necessary to develop an efficient and exact computing method. We adopt a recent general solution strategy for two-stage robust optimization problems, the column-and-constraint generation (CCG) method, to develop an efficient algorithm to compute optimal defensive resources allocation plans. Our study has the following major contributions:

(*i*) The developed algorithm identifies optimal solutions in a reasonable time, which significantly outperforms other existing exact algorithms. Indeed, our algorithm is, to the best of our knowledge, the first algorithm that can efficiently solve a power grid defender-attacker-defender problem on practical instances.

(*ii*) Numerical results indicate that a protection plan, if obtained in an optimal manner, can improve the grid survivability with much less load shed, i.e., optimal protection will always have positive impacts in practice.

(*iii*) Benchmark results of optimal protection plans with respect to those derived by a heuristic procedure and by an attacker-defender model demonstrate the superior performance of optimal protection plans from the defender-attacker-defender model in improving grid survivability.

This chapter is organized as follows. In Section 2.3, we present the tri-level formulation of a defender-attacker-defender model for power grid defensive resources allocation problem. Section 2.4 describes the proposed solution algorithm. Section 2.5 summarizes the relevant numerical results. Finally, a conclusion is provided in Section 2.6.

2.3 Problem Formulation

In this section, we present a tri-level min-max-min formulation for a defender-attacker-defender model for power grid protection on transmission network. Following the convention in [14, 15] etc., we assume that transmission lines are the only components that can be protected or disrupted. Attacks on other components of the transmission system can be modeled according.

Table 1: Nomenclature used in Chapter 2

N	set of indices of buses, indexed by n
J	set of indices of generators, indexed by j
Jn	set of indices of generators connected to bus n
L	set of indices of transmission assets, indexed by l
$o(l)$	origin bus of transmission asset l
$d(l)$	destination bus of transmission asset l
S	budget of attacker on out-of-service transmission assets
R	budget of defender's protection decision
D_n	demand at bus n (in megawatts)
G_j	generation capacity of generator j (in megawatts)
P_l	power flow capacity of transmission line l (in megawatts)
x_l	reactance at line l (Ω)
$\bar{\delta}$	phase angle capacity of connecting bus (rad)
z_l	binary protection decision, 1 if l is protected, and 0 otherwise
v_l	binary attack decision, 0 if line l is attacked, and 1 otherwise
d_n	load shed at node n (in megawatts)
δ_n	phase angle at node n (rad)
g_j	generation level of generator j (in megawatts)
p_l	power flow on line l (in megawatts)

As described in Section 2.2, a tri-level defender-attacker-defender model involves three agents acting sequentially. The top level decisions corresponds to the defender's decisions on allocating defensive resources to protect transmission lines throughout a power grid before any attack is observed. The middle level decisions are made by the terrorist attacker, who seeks to maximize the damage in terms of total load shed of the power system by disconnecting a set of transmission lines. Then, after the disruption by the attacker is observed, the system operator reacts to that disruption by solving an optimal power flow problem to minimize the load shed. The middle-lower level is a typical bi-level power grid interdiction problem. Similar to [11, 12, 14, 15], the optimal power flow problem in the lower level is modeled as a DC optimal power flow model. In the remainder of this chapter, $\hat{\cdot}$ denotes a

fixed decision variable. The formulation of the power grid defender-attacker-defender model is defined in the flowing (2.1)-(2.10).

$$\min_{\mathbf{z}\in\mathbb{Z}} \max_{\mathbf{v}\in\mathbb{V}} \min_{\{p_l, g_j, d_n, \delta_n\}} \sum_{n\in\mathbf{N}} d_n \tag{2.1}$$

$$st. \sum_{l\in\mathbf{L}} z_l \leqslant R \tag{2.2}$$

$$\sum_{l\in\mathbf{L}} (1 - v_l) \leqslant S \tag{2.3}$$

$$p_l x_l = (z_l + v_l - z_l v_l)[\delta_{o(l)} - \delta_{d(l)}],\ \forall l \in \mathbf{L} \tag{2.4}$$

$$\sum_{j\in\mathbf{Jn}} g_j - \sum_{l|o(l)=n} p_l + \sum_{l|d(l)=n} p_l + d_n = D_n, \forall n \in \mathbf{N} \tag{2.5}$$

$$-P_l \leqslant p_l \leqslant P_l,\ \ \forall l \in \mathbf{L} \tag{2.6}$$

$$-\overline{\delta} \leqslant \delta_n \leqslant \overline{\delta},\ \ \forall n \in \mathbf{N} \tag{2.7}$$

$$0 \leqslant g_j \leqslant G_j,\ \ \forall j \in \mathbf{J} \tag{2.8}$$

$$0 \leqslant d_n \leqslant D_n,\ \ \forall n \in \mathbf{N} \tag{2.9}$$

$$v_l, z_l \in \{0, 1\},\ \ \forall l \in \mathbf{L} \tag{2.10}$$

where $\mathbb{Z} = \{\sum_{l\in\mathbf{L}} z_l \leqslant R, z_l \in \{0,1\}, \forall l \in \mathbf{L}\}$ is defender's protection decision set and $\mathbb{V} = \{\sum_{l\in\mathbf{L}}(1 - v_l) \leqslant S, v_l \in \{0,1\}, \forall l \in \mathbf{L}\}$ is attacker's attack decision set. R is the cardinality budget for the defender, which means that the defender could protect up to R transmission lines in a power grid. Similarly, S is the cardinality budget for the attacker so that the attacker can remove up to S transmission lines. Constraints (2.4) capture the active DC power flows on a power grid following the Kirchhoff's Laws with additional protection and

attack decision variables. If line l is protected by the defender, z_l will be set to 1, and then $z_l + v_l - z_l v_l = 1$. Hence, this line will be invulnerable from any attack. If line l is not protected in advance, z_l will be set to 0, which means $z_l + v_l - z_l v_l = v_l$. Then, this line will be subject to attacker's decision during interdiction. Specifically, if $v_l = 0$, i.e., transmission line l is attacked, then the power flow p_l will be zero. Constraints (2.5) preserve power balance at bus n such that the inflow and outflow are equal. Constraints (2.6) simply state that the power flow on line l will be restricted within $[-P_l, P_l]$. Similarly, constraints (2.7) restrict the phase angle of bus n to be within $[-\overline{\delta}, \overline{\delta}]$. Constraints (2.8) bound the power generation of each generator by zero and its capacity. Constraints (2.9) guarantee that the load shed at load bus n do not exceed its nominal demand level and is always nonnegative.

2.4 Solution Methodology

In this section, we describe in details of our customization of the column-and-constraint generation algorithm (CCG) [17] to solve the power grid defender-attacker-defender problem defined in Section 2.3. We refer readers to [17] for a complete proof that the CCG algorithm converges to an optimal solution in finite steps.

The CCG algorithm is implemented at two levels, i.e., a *master problem* (MP) and a *subproblem* (SP). On the one hand, the master problem, which includes a subset of possible attacks, yields a lower bound and a protection plan to the defender-attacker-defender problem. On the other hand, the subproblem, which generates the worst attack plan for a given protection decision, leads to an upper bound. Clearly, when these two bounds merge, we obtain an optimal solution.

2.4.1 Master Problem

Given a set of attack plans $\hat{\mathbf{V}} = \{\hat{\mathbf{v}}^1, \ldots, \hat{\mathbf{v}}^k\} \subseteq \mathbb{V}$, we construct and solve MP to obtain a protection plan. Note that, for a particular attack $\hat{\mathbf{v}}^i$ ($\hat{\mathbf{v}}^i = \{\hat{v}_l^i, \forall l \in \mathbf{L}\}$), we define a set of dispatch variables ($\mathbf{p}^i, \mathbf{g}^i, \mathbf{d}^i, \boldsymbol{\delta}^k$). Then, MP can be constructed as follows.

$$\min_{\mathbf{z}\in\mathbb{Z}} \ \alpha \tag{2.11}$$

$$st. \ \alpha \geqslant \sum_{n\in\mathbf{N}} d_n^i, \ \ \forall i = 1, ..., k \tag{2.12}$$

$$\sum_{l\in\mathbf{L}} z_l \leqslant R \tag{2.13}$$

$$p_l^i x_l = (z_l + \hat{v_l}^i - z_l \hat{v_l}^i)[\delta_{o(l)}^i - \delta_{d(l)}^i], \forall l \in \mathbf{L}, i = 1, ..., k \tag{2.14}$$

$$\sum_{j\in\mathbf{Jn}} g_j^i - \sum_{l|o(l)=n} p_l^i + \sum_{l|d(l)=n} p_l^i + d_n^i = D_n, \forall n \in \mathbf{N}, \forall i = 1, ..., k \tag{2.15}$$

$$-P_l \leqslant p_l^i \leqslant P_l, \ \ \forall l \in \mathbf{L}, \forall i = 1, ..., k \tag{2.16}$$

$$0 \leqslant g_j^i \leqslant G_j, \ \ \forall j \in \mathbf{J}, \forall i = 1, ..., k \tag{2.17}$$

$$0 \leqslant d_n^i \leqslant D_n, \ \ \forall n \in \mathbf{N}, \forall i = 1, ..., k \tag{2.18}$$

$$-\overline{\delta} \leqslant \delta_n^i \leqslant \overline{\delta}, \ \ \forall n \in \mathbf{N}, \forall i = 1, ..., k \tag{2.19}$$

$$z_l \in \{0, 1\}, \ \ \forall l \in \mathbf{L}. \tag{2.20}$$

Note that the constraints (2.14) are nonlinear constraints. By adopting the big-M method, we can easily linearize these coonstraints. Specifically, let M be a sufficiently large real number. For any attack scenario $\hat{\mathbf{v}}^i$, we partition the set of transmission lines into two subsets: attacked lines $\mathbf{L}_\alpha^i$ and lines without attack $\mathbf{L}_\beta^i$, where $\mathbf{L}_\alpha^i = \{l|\hat{v}_l^i = 0, l \in \mathbf{L}\}$ and

$\mathbf{L}^i_\beta = \{l|\hat{v}^i_l = 1, l \in \mathbf{L}\}$. For the attacked transmission lines ($l \in \mathbf{L}^i_\alpha$), (2.14) are replaced by a set of following constraints:

$$p^i_l x_l - [\delta^i_{o(l)} - \delta^i_{d(l)}] \leqslant M(1 - z_l), \ \ \forall l \in \mathbf{L}^i_\alpha \tag{2.21}$$

$$p^i_l x_l - [\delta^i_{o(l)} - \delta^i_{d(l)}] \geqslant M(z_l - 1), \ \ \forall l \in \mathbf{L}^i_\alpha \tag{2.22}$$

$$-P_l z_l \leqslant p^i_l \leqslant P_l z_l, \ \ \forall l \in \mathbf{L}^i_\alpha. \tag{2.23}$$

For the lines without attack ($l \in \mathbf{L}^i_\beta$), (2.14) are replaced by $p^i_l x_l = \delta^i_{o(l)} - \delta^i_{d(l)}, \ \ \forall l \in \mathbf{L}^i_\beta$. As a result, MP, which is a single level mixed-integer programming problem, can be readily solved by a professional mixed-integer programming (MIP) solver. We point it out that because $\hat{\mathbf{V}}$ is a subset of $\mathbb{V}$, compared to the complete defender-attacker-defender model formation in (2.1)-(2.9), MP is a relaxation and, therefore, provides a lower bound value.

2.4.2 Subproblem

Subproblem serves the function to identify the worst-case attack plan for a given protection decision. Hence, given protection plan $\hat{\mathbf{z}}$, where $\hat{\mathbf{z}} = \{\hat{z}_l = 0 \ or \ 1, \forall l \in \mathbf{L}\}$, the corresponding subproblem is the following bi-level max-min problem.

$$\max_{\mathbf{v} \in \mathbb{V}} \min_{\{p_l, g_j, d_n, \delta_n\}} \sum_{n \in \mathbf{N}} d_n \tag{2.24}$$

$$st. \ \sum_{l \in \mathbf{L}} (1 - v_l) \leqslant S \tag{2.25}$$

$$p_l x_l - (\hat{z}_l + v_l - \hat{z}_l v_l)[\delta_{o(l)} - \delta_{d(l)}] = 0, \ \ \forall l \in \mathbf{L} \tag{2.26}$$

$$-P_l \leqslant p_l \leqslant P_l, \ \ \forall l \in \mathbf{L} \tag{2.27}$$

$$\sum_{j\in\mathbf{Jn}} g_j - \sum_{l|o(l)=n} p_l + \sum_{l|d(l)=n} p_l + d_n = D_n, \forall n \in \mathbf{N} \tag{2.28}$$

$$0 \leqslant g_j \leqslant G_j, \ \ \forall j \in \mathbf{J} \tag{2.29}$$

$$0 \leqslant d_n \leqslant D_n, \ \ \forall n \in \mathbf{N} \tag{2.30}$$

$$-\overline{\delta} \leqslant \delta_n \leqslant \overline{\delta}, \ \ \forall n \in \mathbf{N} \tag{2.31}$$

$$v_l \in \{0,1\}, \ \ \forall l \in \mathbf{L}. \tag{2.32}$$

Based on a given protection plan $\hat{\mathbf{z}}$, the transmission lines can be divided into two subsets: unprotected lines $\mathbf{L}_a$ and protected lines $\mathbf{L}_b$, where $\mathbf{L}_a = \{l|\hat{z}_l = 0, l \in \mathbf{L}\}$ and $\mathbf{L}_b = \{l|\hat{z}_l = 1, l \in \mathbf{L}\}$. For the unprotected lines in $\mathbf{L}_a$, (2.26) and (2.27) are replaced by a set of constraints (2.33)-(2.35):

$$p_l x_l - \left[\delta_{o(l)} - \delta_{d(l)}\right] \leqslant M(1 - v_l), \ \ \forall l \in \mathbf{L}_a \tag{2.33}$$

$$p_l x_l - \left[\delta_{o(l)} - \delta_{d(l)}\right] \geqslant M(v_l - 1), \ \ \forall l \in \mathbf{L}_a \tag{2.34}$$

$$-P_l v_l \leqslant p_l \leqslant P_l v_l, \ \ \forall l \in \mathbf{L}_a. \tag{2.35}$$

For the protected lines in $\mathbf{L}_b$, (2.26) and (2.27) are replaced by the following constraints (2.36)-(2.37):

$$p_l x_l = \delta_{o(l)} - \delta_{d(l)}, \ \ \forall l \in \mathbf{L}_b \tag{2.36}$$

$$-P_l \leqslant p_l \leqslant P_l, \ \ \forall l \in \mathbf{L}_b. \tag{2.37}$$

Since the lower level problem of subproblem is a single level minimization linear program and always feasible for any attack, through strong duality, we obtain a single level maximization problem (2.38)-(2.50). In the following formulation (2.38)-(2.50), λ_n is the dual variable for (2.28), γ_j is the dual variable for (2.29), α_n is the dual variable for (2.30), ξ_n and χ_n are the dual variables for (2.31), β_l and τ_l are the dual variables for (2.33) and (2.34), θ_l and ρ_l are dual variables for (2.35), μ_l is the dual variable for (2.36), ϕ_l and φ_l are the dual variables for (2.37).

$$\max \sum_{l\in\mathbf{L}_b} P_l(\phi_l - \varphi_l) + \sum_{l\in\mathbf{L}_a} M(1-v_l)(\beta_l - \tau_l)$$

$$+\sum_{j\in\mathbf{J}} G_j\gamma_j + \sum_{n\in\mathbf{N}} \overline{\delta}(\xi_n - \chi_n) + \sum_{n\in\mathbf{N}} D_n\alpha_n + \sum_{l\in\mathbf{L}_a} P_l(\theta_l - \rho_l)v_l \tag{2.38}$$

$$st.\ \sum_{l\in\mathbf{L}}(1-v_l) \leqslant S \tag{2.39}$$

$$\mu_l + \phi_l + \varphi_l - \lambda_{n|o(l)=n} + \lambda_{n|d(l)=n} = 0, \forall l \in \mathbf{L}_b \tag{2.40}$$

$$\beta_l + \tau_l + \theta_l + \rho_l - \lambda_{n|o(l)=n} + \lambda_{n|d(l)=n} = 0, \forall l \in \mathbf{L}_a \tag{2.41}$$

$$\gamma_j + \lambda_{n|j\in\mathbf{Jn}} \leqslant 0,\ \ \forall j \in \mathbf{J} \tag{2.42}$$

$$\sum_{l\in\mathbf{L}_b,d(l)=n} \mu_l - \sum_{l\in\mathbf{L}_b,o(l)=n} \mu_l - \sum_{l\in\mathbf{L}_a,o(l)=n} (\beta_l + \tau_l) + \sum_{l\in\mathbf{L}_a,d(l)=n} (\beta_l + \tau_l) +$$

$$(\chi_n + \xi_n)x_l = 0,\ \ \forall n \in \mathbf{N} \tag{2.43}$$

$$\lambda_n + \alpha_n \leqslant 1,\ \ \forall n \in \mathbf{N} \tag{2.44}$$

$$v_l \in \{0,1\},\quad \forall l \in \mathbf{L} \tag{2.45}$$

$$\gamma_j \leqslant 0,\ \ \forall j \in \mathbf{J} \tag{2.46}$$

$$\xi_n \leqslant 0, \alpha_n \leqslant 0, \quad \forall n \in \mathbf{N} \tag{2.47}$$

$$\chi_n \geqslant 0, \lambda_n \ free, \quad \forall n \in \mathbf{N} \tag{2.48}$$

$$\beta_l \leqslant 0, \theta_l \leqslant 0, \tau_l \geqslant 0, \rho_l \geqslant 0, \quad \forall l \in \mathbf{L}_a \tag{2.49}$$

$$\mu_l \ free, \phi_l \leqslant 0, \varphi_l \geqslant 0, \quad \forall l \in \mathbf{L}_b \tag{2.50}$$

Again, since v_l is a binary variable, linearization of the nonlinear terms in (2.38) can be obtained by using the big-M method. Thus, we obtain the linearized formulation of SP. Hence, subproblem can also be solved by a professional MIP solver.

2.4.3 Algorithm Implementation

Next, we present the implementation steps of our CCG algorithm as demonstrated in Algorithm 1. The optimality tolerance gap of our algorithm is ϵ.

2.5 Computational Study

We apply our method to the IEEE one-area RTS-1996 system [18]. This system consists of 24 buses, 38 lines, 32 generators, and 17 loads, as illustrated in Figure 1. Circuits sharing the same towers are treated as independent lines. The algorithm is implemented with CPLEX 12.4 in C++ on top of an Intel dual core 3.00GHz, 4GB memory PC. The optimality tolerance gap ϵ is set at 0.1%. As an example, an optimal solution for the defender-attacker-defender model with protection budget $R = 2$ and attack budget $S = 3$ is illustrated in Figure 1. The best protection plan, in this case, is to protect transmission line 14-16 and 16-17. We present the optimal load shed vaules and computational time for all instances with attack budget $S = 1$ to 12 and protection budget $R = 0$ to 4 in Table 2 and Table 3, respectively.

Algorithm 1 : Algorithm Implementation for DAD

1: Initialization: set the lower bound $LB = -\infty$, the upper bound $UB = \infty$, and the set of attack plan $\hat{\mathbf{V}}$ to be empty with iteration index $k = 1$.

2: **while** gap $\geqslant \epsilon$ **do**

3: Solve MP (2.11)-(2.20), obtain its optimal value $objMP$ and a protection decision $\hat{\mathbf{z}}$, and update LB with $objMP$.

4: Solve subproblem(2.38)-(2.50), obtain its optimal value $objSP$ and an optimal attack $\hat{\mathbf{v}}^k$. Then, update $UB = min\{UB, objSP\}$, add $\hat{\mathbf{v}}^k$ to $\hat{\mathbf{V}}$, create dispatch variables $(\mathbf{p}^k, \mathbf{g}^k, \mathbf{d}^k, \boldsymbol{\delta}^k)$, and add the following constraints to MP:

$$\alpha \geqslant \sum_{n \in \mathbf{N}} d_n^k$$

$$p_l^k x_l - [\delta_{o(l)}^k - \delta_{d(l)}^k] \leqslant M(1 - z_l), \forall l \in \mathbf{L}_\alpha^k \tag{2.51}$$

$$p_l^k x_l - [\delta_{o(l)}^k - \delta_{d(l)}^k] \geqslant M(z_l - 1), \forall l \in \mathbf{L}_\alpha^k \tag{2.52}$$

$$-P_l z_l \leqslant p_l^k \leqslant P_l z_l, \ \ \forall l \in \mathbf{L}_\alpha^k \tag{2.53}$$

$$p_l^k x_l = \delta_{o(l)}^k - \delta_{d(l)}^k, \ \ \forall l \in \mathbf{L}_\beta^k \tag{2.54}$$

$$-P_l \leqslant p_l^k \leqslant P_l, \ \ \forall l \in \mathbf{L}_\beta^k \tag{2.55}$$

$$\sum_{j \in \mathbf{Jn}} g_j^k - \sum_{l|o(l)=n} p_l^k + \sum_{l|d(l)=n} p_l^k + d_n^k = D_n, \forall n \in \mathbf{N} \tag{2.56}$$

$$0 \leqslant g_j^k \leqslant G_j, \ \ \forall j \in \mathbf{J} \tag{2.57}$$

$$0 \leqslant d_n^k \leqslant D_n, \ \ \forall n \in \mathbf{N} \tag{2.58}$$

$$-\overline{\delta} \leqslant \delta_n^k \leqslant \overline{\delta}, \ \ \forall n \in \mathbf{N}. \tag{2.59}$$

5: update gap $(UB - LB)/LB$, $k \leftarrow k + 1$.

6: **end while**

7: **return** $\mathbf{z}^* \leftarrow \hat{\mathbf{z}}$. ■

As can be seen from Table 2, for each column of Table 2, the load shed is non-decreasing with the increase of attack budget S. Indeed, this observation reveals that the attacker could cause more damage to a power grid with more available attacking resources . For each row in the same table, the load shed is non-increasing with an increasing protection budget R except for the cases with anticipated attack budget to be 1, i.e., $S = 1$. This observation reveals that adding defensive resources will improve power grid survivability during attacks.

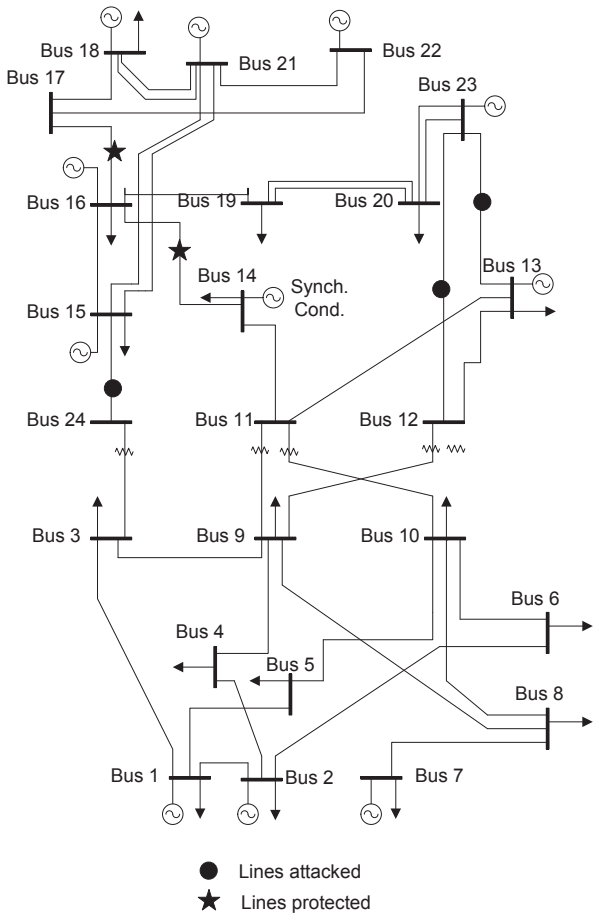

Figure 1: Reliability test system and a solution

2.5.1 Computational Efficiency

Our algorithm demonstrates a superior computational performance over the other exact algorithm in [15], especially for complicated cases, i.e., those with the relatively larger attack or protection budgets. Figure 2 presents the computational time (averaged over R from 0 to 4) of our algorithm compared with those made by the implicit enumeration method in [15], which are generated on a Sun Fire X4140 X64 with 2 processors at 2.3 GHz and 8GB RAM using MATLAB/CPLEX 11.0 under GAMS. Note that the computation time of the implicit

Table 2: Load shed (MW) for an IEEE system

S	$R=0$	$R=1$	$R=2$	$R=3$	$R=4$
1	0	0	0	0	0
2	194	151	136	118	118
3	618	571	422	377	266
4	922	733	618	571	492
5	1037	843	733	673	571
6	1057	969	788	731	676
7	1278	1057	898	808	761
8	1393	1265	1013	885	770
9	1413	1285	1013	885	825
10	1448	1320	1068	940	849
11	1468	1340	1103	975	927
12	1532	1404	1218	1052	927

enumeration method increases almost exponentially to over 2000 seconds with the budget of interdicted lines (S) from 1 to 12. On the contrary, the computation time of column-and-constraint generation algorithm increases at a much slower rate and is much less sensitive to attack budget S.

2.5.2 Effectiveness of Optimal Protection

To investigate the effectiveness of allocating defensive resources based on the defender-attacker-defender model, we conduct experiments with different protection and attack budgets. Figure 3 presents the load shed of the power grid under different protection and attack budgets. Note that, as a general rule, the benefit of protecting transmission assets is always positive. When the attack budget S is small, e.g., less than 2 lines are attacked, such a benefit may not be large, which concurs an observation made in Bier et al. [14] that protection may not be cost-effective. However, when S becomes larger, e.g., $S \geqslant 3$, the benefit of protection becomes very significant. Indeed, when the protection budget R is set to 2,

Table 3: Computation time (second) for an IEEE system

S	$R=0$	$R=1$	$R=2$	$R=3$	$R=4$
1	0.15	0.12	0.14	0.17	0.25
2	0.45	0.75	1.13	1.54	2.36
3	0.75	1.40	2.67	3.30	5.45
4	1.61	2.52	5.47	10.19	7.29
5	5.50	8.76	17.98	21.40	40.83
6	11.25	20.52	28.69	65.50	88.25
7	16.69	28.32	75.07	113.97	246.82
8	10.09	36.19	74.30	191.33	108.11
9	32.73	84.33	154.69	196.03	632.63
10	10.99	44.34	69.01	199.20	517.46
11	24.79	53.11	157.64	243.46	423.58
12	12.65	16.60	59.99	144.23	323.68

Table 4: Comparison between AD and DAD

S	No protection load shed (MW)	AD		DAD (R=S)	
		protected lines	load shed (MW)	protected lines	load shed (MW)
1	0	None	0	None	0
2	194	11-14, 14-16	151	14-16, 17-22	136
3	618	15-21A, 15-21B,16-17	571	13-23, 14-16,16-17	377
4	922	3-24,12-23, 13-23,14-16	733	12-23,14-16, 16-17,17-22	492

i.e., up to two lines can be protected, it is typical that more than 25% of load shed can be reduced under various attack scenarios. When the protection budget rises up to 4, the total load shed reduction can be as much as 57%.

In an empirical study of their fast hardening method, Bier et al. [14] note that hardening, i.e., protection, could have a negative impact on the system. They believe it is probably due to the non-optimal nature of the Max Line interdiction algorithm, which is a subroutine used to derive attack and hardening decisions and to evaluate the hardening solutions. By

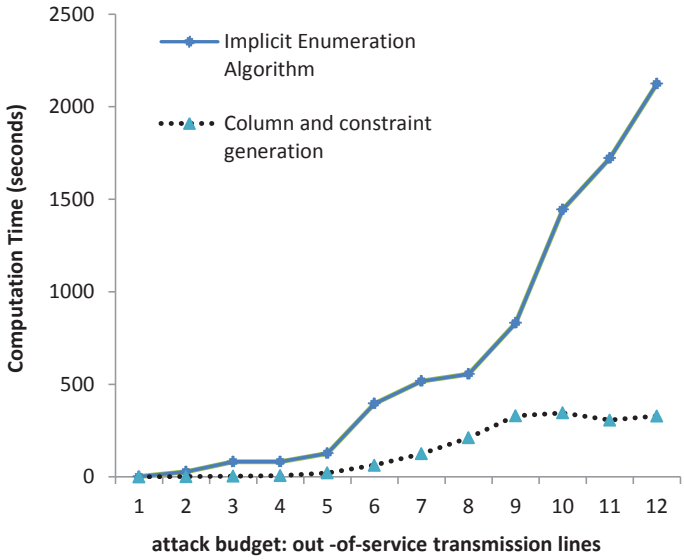

Figure 2: Comparison of computational time

benchmark the hardening solutions with optimal protection plans, we believe that it can identify the true reason behind and assess the performance of the hardening method.

We implement the hardening method and evaluate the hardening solutions by the Max Line interdiction algorithm [14]. Results are represented by dashed lines in Figure 4 where protection budget is set as 2 and 4, respectively. H2 and H4 stand for the results with 2 lines and 4 lines hardened respectively, obtained by setting the Max Line interdiction iteration limit to 15, the hardening iteration to 1 and 2, respectively, and the hardening batch size to 2 [14]. As can be seen in Figure 4, if attack budget S equals to 4 (or 5 or 6), load sheds of H4 are more than those of H2, whereas H4 has 4 lines protected and H2 only has 2 lines protected. Such a result indicates that hardening could have a negative impact by incurring more load shed. However, if optimal attack plans are used for evaluation, whose results are represented by solid lines in Figure 4, we observe that hardening does not cause

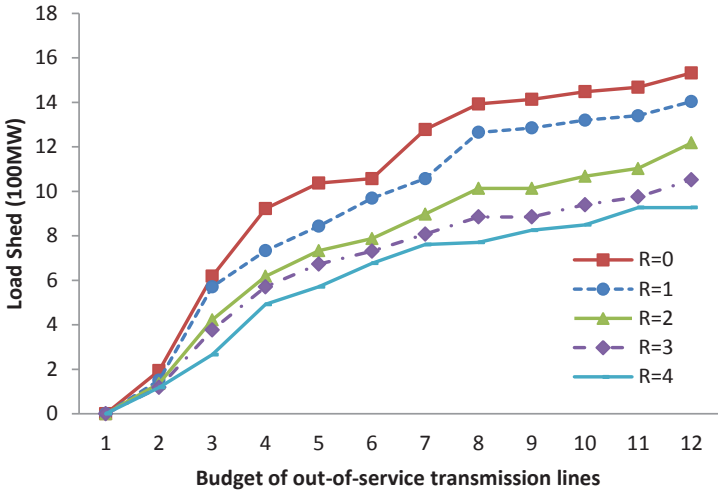

Figure 3: Load shed with different protection budgets

a negative impact under any attack scenario and it actually reduces load sheds in general. Hence, because of the non-optimal nature of the Max Line interdiction algorithm, it can not provide a proper evaluation to justify the quality of hardening solutions. This result confirms the conjecture in [14] that the heuristic nature of that algorithm could lead to the incorrect conclusion. Figure 5 presents the load shed of hardening solutions H2 and H4 (under optimal attack plans) and those of optimal protection plans with the same protection budgets. Clearly, although hardening solutions help to improve power grid survivability, they are significantly less effective compared to optimal protection plans. Especially, when the attack budget S is large, protection by a hardening solution could cause the grid to carry almost 70% more total load shed than that by an optimal one.

2.5.3 Attacker-Defender versus Defender-Attacker-Defender

It is mentioned in [11] and [12] that, with the same protection budget, a protection plan based on a defender-attacker-defender model is more effective than that of an attacker-

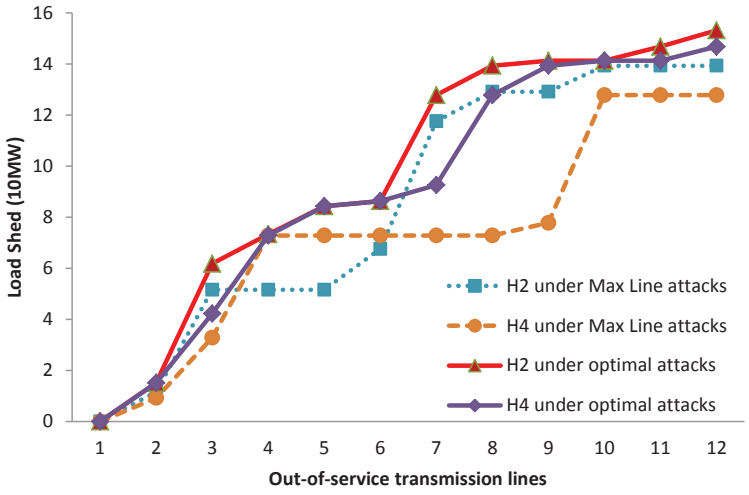

Figure 4: Performance of another hardening method

defender model when a system is under contingency. To verify this observation, we conduct a study to compare the protection plans from the attacker-defender model and the defender-attacker-defender model. The attacker-defender model is obtained by setting protection budget to zero and fixing all protection variables to zero in formulation (2.1)-(2.9). System load sheds of no protection and of different protection plans are computed under worst-case interdiction with attack budget S from 1 to 4. Specifically, load shed of no protection scenario is obtained from the attacker-defender model directly. The protection plan from the attacker-defender model is the set of transmission lines in the most destructive interdiction plan, which is the optimal solution of the attacker-defender model. After forcing those critical components to be protected, we solve the attacker-defender model again to obtain load shed. The load shed of optimal protection plans is simply obtained by solving the defender-attacker-defender model with $R = S$. Table 4 presents the protection plans and load shed. As can be seen, even though both the attacker-defender model and the defender-attacker-defender

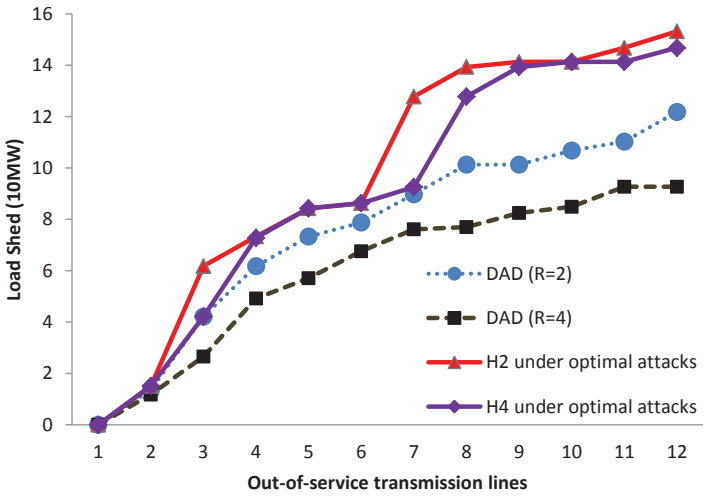

Figure 5: Comparison between solutions

model improve power grid survivability by reducing the system load shed under contingency, the attacker-defender model fails to derive the optimal protection plan and leads to more total load shed than that of the defender-attacker-defender model. Actually, the protection plans from the attacker-defender model could cause 50% more load shed, compared to the optimal protection plans from the defender-attacker-defender model. This result not only confirms the observations made by Brown et al. [11] and Yao et al. [12], but also further highlights the drastic difference between the attacker-defender model and the defender-attacker-defender model. In fact, based on results in Table 4, as well as Figure 4-5, we provide the following remarks. First of all, if we do not have the capability to identify most destructive attack plans of an attacker, neither can we properly evaluate or derive effective protection plans. Secondly, an exact protection plan from the defender-attacker-defender model demonstrates superior performance with much less load shed, compared to those derived by heuristic methods or the attacker-defender model.

Hence, given that huge economic losses and serious infrastructure damages will be incurred under a power grid disruption, it is of a particular value to apply defender-attacker-defender model and solutions in system planning and operations.

2.6 Conclusion

This chapter presents a new approach to solve a power grid defender-attacker-defender model. The proposed column-and-constraint generation algorithm finds the optimal protection plan within acceptable computational time, which significantly outperforms the existing exact solution method. Case studies on the IEEE one-area RTS-1996 system have been done to verify the effectiveness of optimally allocating defensive resources to hedge against terrorist attacks.

CHAPTER 3: DEFENDER-ATTACKER-DEFENDER MODEL WITH NETWORK TOPOLOGY CONTROL

3.1 Background

Power system vulnerability is a serious concern to power industry and the whole society. Terrorists and natural disasters' attacks on power grids are regarded as a national threat due to their massive damage. A recent report released by National Research Council emphasizes that a terrorist attack on U.S. power grids could be much more destructive than Hurricane Sandy because it could black out large segments of the country for months, cause hundreds of billions of economic damage, and lead to thousands of deaths [2]. Hence, protecting or hardening grid components against various disruptions is of a high national interest [19, 20]. Moreover, [21] clearly states that energy security efforts should start with hardening power grids.

To derive an effective plan that protects critical components with limited defensive resources, researchers often adopt game theory models to simulate the interaction between system operators and terrorists/natural disasters. Among them, defender-attacker-defender models are probably the most popular ones [1, 12–14, 22]. In those DAD models, system operators protect or harden grid components before any possible attack. Then, given the grid with some components non-attackable, attackers seek to destroy other critical components with the maximized total load shed. Once the attack happens, system operators respond

to the disruptions by taking mitigation operations, for example, re-dispatching power flows, to minimize the load shed. Because those models are challenging tri-level mixed-integer programming problems, many research efforts focus on developing fast algorithms to solve practical instances. Examples include heuristic methods [11, 14] and exact algorithms [1, 22].

According to [1], it is critical to understand and model the defender's mitigation capability as it affects the attacker's attacking targets. Without a full description of the attacker's behaviors, the optimality of the protection plan will be forfeited. Nevertheless, to the best of our knowledge, all existing research on power grid defender-attacker-defender models neglect one important mitigation operation: transmission line switching (also known as topology control).

In fact, given that expanding transmission infrastructure is very costly and could pose many integration issues to existing power grids, the Federal Energy Regulatory Commission (FERC) orders call for improved economic operations of the electric transmission network. Especially, those orders promote the use of transmission line switching, which changes the transmission network topology, to improve utilization of existing transmission systems. Actually, transmission line switching has been included in real operations as a corrective mechanism to alleviate line overloads and voltage violations after contingencies [23–26]. For example, PJM has incorporated the post-contingency transmission line switching actions into its Special Protection Schemes (SPSs) [27], which reflects a shift from the preventive approach to a more economic corrective approach. The ISO New England studies the dispatch efficiency along with reliability requirements to determine the optimal periods to take

off transmission lines for maintenance and earns a saving of 72.5 million dollars in 2008 [27]. Based on these current industry practices, it is believed that transmission line switching should be deeply investigated and effectively utilized.

To analytically study transmission line switching operations, [28] considers the optimal transmission line switching problem by introducing transmission line switching decision into a DC optimal power flow model. According to [28], a saving of 25% in dispatch costs can be achieved from transmission line switching. Recent work [29] also reveals the significant benefits of transmission line switching in utilizing wind power. Transmission line switching is also introduced to power system vulnerability analysis as system operator's post-contingency operations [5, 10, 30]. Given that transmission line switching can greatly improve dispatch capability of a power system, in this chapter, we consider protection operations and transmission line switching decisions under the defender-attacker-defender model. We expect to derive cost-effective protection plans that can better use limited defensive resources.

However, the challenge from incorporating transmission line switching is not only reflected in how to model this operation in the defender-attacker-defender framework, but also in how to solve the new model. All existing algorithms for general defender-attacker-defender models depend on the strong duality of the inner most linear programming problem, which is not the case when binary transmission line switching decisions are included. To address this challenge, we adopt the nested column-and-constraint generation (NCCG) algorithm [31] that extends the basic column-and-constraint method and is designed specifically to deal with the tri-level problem with an inner most mixed-integer problem.

The rest of this chapter is organized as follows. In Section 3.2, we give the formulation of the defender-attacker-defender model with transmission line switching as post-contingency operations (i.e., DAD-TLS formulation) and present some structural properties. Section 3.3 describes the customized nested column-and-constraint generation algorithm to solve DAD-TLS formulation. Section 3.4 shows our computational results. In Section 3.5, we analyze the benefits from introducing transmission line switching operations to hardening decisions. Section 3.6 concludes with a discussion.

3.2 Problem Formulation

In this section, we present a tri-level min-max-min formulation of a defender-attacker-defender model for power grid protection problem that includes transmission line switching as a mitigation strategy. Similar formulations without transmission line switching can be found in [1, 12, 15].

3.2.1 Modeling Protection, Attack, and Transmission Switching

A study in [28] initially formulates transmission line switching operation into a DC optimal power flow model to enable the system operators change the topology of transmission network. Transmission line switching is represented by a binary variable, which takes effect on the Kirchhoff's law constraints. Similarly, our study considers transmission line switching as a corrective post-contingency/attack operation and employs binary transmission line switching variables in the inner DC optimal power flow model. This will allow the operator to modify the transmission system network topology along with the power flow related variables. Specifically, each transmission line l is associated with a binary variable

Table 5: Nomenclature used in Chapter 3

$\mathbf{N}$	set of indices of buses
$\mathbf{J}$	set of indices of generators
$\mathbf{L}$	set of indices of transmission lines
j	generator index, $j \in \mathbf{J}$
l	transmission line index, $l \in \mathbf{L}$
n	bus index, $n \in \mathbf{N}$
$\mathbf{Jn}$	set of indices of generators connected to bus n
$o(l)$	origin bus of transmission line l
$d(l)$	destination bus of transmission line l
$\mathbb{Z}$	defender's protection decision set
$\mathbb{V}$	attacker's attack decision set
K	budget for attacker's disruption
R	budget for defender's protection
x_l	reactance at line l
D_n	demand at bus n
G_j	generation capacity of generator j
P_l	power flow capacity of transmission line l
z_l	protection decision, 1 for protected, 0 otherwise
v_l	attack decision, 0 for attacked, 1 otherwise
w_l	transmission line switching, 0 for switched off, 1 otherwise
d_n	load shed at node n
δ_n	phase angle at node n
g_j	generation level of generator$j$
p_l	power flow on line l
$\mathbf{z}$	vector of $z_l, \forall l \in L$, a protection plan
$\mathbf{v}$	vector of $v_l, \forall l \in L$, an attack plan
$\mathbf{w}$	vector of $w_l, \forall l \in L$, a transmission line switching plan
$\hat{*}$	fixed decision variable (or vector) of $*$

w_l that represents whether a line is included in the system ($w_l = 1$) or disconnected (i.e., transmission line is switched off and $w_l = 0$). Hence, the Kirchhoff's law constraints in the defender-attacker-defender model with transmission line switching can be formulated as equation (3.1).

$$p_l x_l = w_l(z_l + v_l - z_l v_l)[\delta_{o(l)} - \delta_{d(l)}],\ \forall l \in \mathbf{L} \tag{3.1}$$

In (3.1), $(z_l + v_l - z_l v_l)$ represents the logic of protection (z_l) and attack (v_l) decisions. If $z_l = 1$, line l is protected, then no attack on that line would be possible since $z_l + v_l - z_l v_l = z_l = 1$. Note that if a transmission line is out-of-service after an attack, it must be non-protected $(\hat{z}_l = 0)$ and attacked $(\hat{v}_l = 0)$, which means $z_l + v_l - z_l v_l = 0$, and power flow p_l is zero. If a transmission line is not attacked $(\hat{v}_l = 1)$, (3.1) reduces to $p_l x_l = w_l[\delta_{o(l)} - \delta_{d(l)}]$. Thus, transmission variable w_l will take effect on the transmission line.

3.2.2 Defender-Attacker-Defender with Transmission Switching

The tri-level defender-attacker-defender model involves three agents acting sequentially. The top level corresponds to the defender's decision on allocating defensive resources to protect transmission lines throughout a power grid. The middle level decisions are controlled by an attacker, who seeks to maximize the total load shed of the power system by disconnecting a set of transmission lines that are unprotected. Then, after the disruption by the attacker is observed, the system operator reacts to that disruption by solving an optimal power flow problem with transmission line switching as a network topology control method to minimize the total load shed. Hence, the inner most problem is a mixed-integer program. It differs from those in [1, 11, 12, 14, 15, 32] where the inner most level is simply a linear program for linear DC optimal power flow.

The mixed-integer nonlinear programming (MINLP) formulation of the defender-attacker-defender model with transmission line switching (DAD-TLS) is:

$$\min_{\mathbf{z}\in\mathbb{Z}} \max_{\mathbf{v}\in\mathbb{V}} \min_{\{w_l, p_l, g_j, d_n, \delta_n\}} \sum_{n\in\mathbf{N}} d_n \tag{3.2}$$

$$st. \sum_{l \in \mathbf{L}} z_l \leqslant R \tag{3.3}$$

$$\sum_{l \in \mathbf{L}} (1 - v_l) \leqslant K \tag{3.4}$$

$$p_l x_l = w_l (z_l + v_l - z_l v_l)[\delta_{o(l)} - \delta_{d(l)}], \ \forall l \in \mathbf{L} \tag{3.5}$$

$$\sum_{j \in \mathbf{Jn}} g_j - \sum_{l|o(l)=n} p_l + \sum_{l|d(l)=n} p_l + d_n = D_n, \forall n \in \mathbf{N} \tag{3.6}$$

$$-P_l \leqslant p_l \leqslant P_l, \ \ \forall l \in \mathbf{L} \tag{3.7}$$

$$0 \leqslant g_j \leqslant G_j, \ \ \forall j \in \mathbf{J} \tag{3.8}$$

$$0 \leqslant d_n \leqslant D_n, \ \ \forall n \in \mathbf{N} \tag{3.9}$$

$$v_l, z_l, w_l \in \{0, 1\}, \ \ \forall l \in \mathbf{L} \tag{3.10}$$

where $\mathbb{Z} = \{\sum_{l \in \mathbf{L}} z_l \leqslant R, z_l \in \{0,1\}, \forall l \in \mathbf{L}\}$ is defender's protection decision set, and $\mathbb{V} = \{\sum_{l \in \mathbf{L}} (1 - v_l) \leqslant K, v_l \in \{0,1\}, \forall l \in \mathbf{L}\}$ is attacker's attack decision set. R is the cardinality budget for the defender, which means the defender can protect up to R transmission lines. Similarly, K is the cardinality budget for the attacker so that the attacker can remove up to K transmission lines. Note that it is consistent with N-K reliability consideration. Constraints (3.5) capture the active DC power flows on a power grid following the Kirchhoff's Law with protection, attack, and transmission line switching decision variables. Constraints (3.6) preserve power flow balance at bus n. Constraints (3.7) simply state that the power flow on line l will be restricted within $[-P_l, P_l]$. Constraints (3.8) bound the power generation of each generator by zero and its capacity. Constraints (3.9) guarantee that the load shed at load bus n does not exceed its nominal demand and is always nonnegative. Note that,

because of the binary transmission line switching variables, the inner most optimal power flow problem with transmission line switching becomes a mixed-integer program. All existing exact algorithms in solving defender-attacker-defender models, e.g., the implicit enumeration in [15], the column-and-constraint generation in [1], are no longer applicable as they depends on the duality theory of linear program.

3.2.3 Structural Properties

In this subsection, we present some insights and properties of DAD-TLS formulation presented in (3.2-3.10). Let $f_{(R,K)}$ represents the optimal value for a given hardening budget R and a given attack budget K. The next result follows easily by analyzing the relaxation relationship between different Rs (and Ks).

THEOREM 1 *$f_{(R,K)}$ is non-increasing in R and non-decreasing in K.*

Proof: Indeed, it is easy to see that it is only necessary to consider cases where $R+K \leqslant |L|$. Otherwise, we can reduce K to $(|L| - R)$, given that extra attack efforts are useless. Let $f_{(R,K)}(\hat{\mathbf{z}})$ be the optimal value for a given protection plan $\hat{\mathbf{z}}$ and $\hat{\mathbf{v}}$ be its corresponding optimal attack plan. By an abuse of notation, we also use $\hat{\mathbf{z}}$ (and $\hat{\mathbf{v}}$, respectively) to represent the set of associated transmission lines subject to protection (and attack, respectively).

THEOREM 2 (Intersection Theorem)

1. *$\hat{\mathbf{z}} \cap \hat{\mathbf{v}} = \varnothing$, i.e., an optimal attack plan does not involve any transmission lines under protection;*

2. *For a protection plan $\mathbf{z}^0$, if $\mathbf{z}^0 \cap \hat{\mathbf{v}} = \varnothing$, we have $f_{(R,K)}(\mathbf{z}^0) \geqslant f_{(R,K)}(\hat{\mathbf{z}})$. Therefore, unless*

$\hat{\mathbf{z}}$ is an optimal protection plan to DAD-TLS problem, it is necessary to have $\mathbf{z}^0 \cap \hat{\mathbf{v}} \neq \varnothing$ if $\mathbf{z}^0$ is an improved protection plan over $\hat{\mathbf{z}}$.

Proof: Note that the first statement follows easily. Also, it is sufficient to prove the first part of the second statement. So, we have

$$\begin{aligned} & f_{(R,K)}(\mathbf{z}^0) \\ = & \max_{\mathbf{v}\in\mathbb{V}} \Big\{ \min \sum_{n\in\mathbf{N}} \mathbf{d}_n : (3.4)-(3.10), \mathbf{z}=\mathbf{z}^0 \Big\} \\ \geqslant & \Big\{ \min \sum_{n\in\mathbf{N}} \mathbf{d}_n : (3.5)-(3.10), \mathbf{z}=\mathbf{z}^0, \mathbf{v}=\hat{\mathbf{v}} \Big\} \end{aligned}$$

Because $\hat{\mathbf{z}} \cap \hat{\mathbf{v}} = \mathbf{z}^0 \cap \hat{\mathbf{v}} = \varnothing$, it is easy to see that

$$\begin{aligned} & \Big\{ \min \sum_{n\in\mathbf{N}} \mathbf{d}_n : (3.5)-(3.10), \mathbf{z}=\mathbf{z}^0, \mathbf{v}=\hat{\mathbf{v}} \Big\} \\ = & \Big\{ \min \sum_{n\in\mathbf{N}} \mathbf{d}_n : (3.5)-(3.10), \mathbf{z}=\hat{\mathbf{z}}, \mathbf{v}=\hat{\mathbf{v}} \Big\} \\ = & f_{(R,K)}(\hat{\mathbf{z}}) \end{aligned}$$

Therefore, we have $f_{(R,K)}(\mathbf{z}^0) \geqslant f_{(R,K)}(\hat{\mathbf{z}})$.

3.3 Solution Methodology

In this section, we customize and implement the nested column-and-constraint generation algorithm in [31] to solve the DAD-TLS. In particular, by extending the inner most mix integer optimal power flow problem (with transmission line switching) into a bi-level program, the middle and inner levels' problem becomes a tri-level problem where the inner most is a linear program. Then, based on the strong duality, we can further convert that

tri-level formulation into a max-min-max format. Specifically, for a given protection plan $\hat{\mathbf{z}}$, we have

$$\max_{\mathbf{v}\in\mathbb{V}} \min_{\{w_l,p_l,g_j,d_n,\delta_n\}} \sum_{n\in\mathbf{N}} d_n = \max_{\mathbf{v}\in\mathbb{V}} \min_{w_l} \min_{\{p_l,g_j,d_n,\delta_n\}} \sum_{n\in\mathbf{N}} d_n = \max_{\mathbf{v}\in\mathbb{V}} \min_{w_l} \max_{\{\pi^1,\ldots,\pi^6\}} \beta$$

where β is the dual objective function, (π^1, π^2) are the dual variables for the constraints (3.5) and (3.6), (π^3, π^4) are the dual variables for constraints (3.7), π^5 is the dual variable for constraints (3.8) and π^6 is the dual variable for constraints(3.9). Given this max-min-max problem, we can solve it by the column-and-constraint generation algorithm to derive the optimal attack plan $\mathbf{v}^*$. Then, with the $\mathbf{v}^*$, we can again make use of the column-and-constraint generation algorithm to solve the complete defender-attacker-defender model in (3.2-3.10).

Therefore, the column-and-constraint method is used in two levels, for which the whole procedure is called nested column-and-constraint method. To distinguish the master problems and sub problems of those two levels, we denote the master problem of outer level as NCCG master problem, the inner level master problem as CCG master problem, and the inner level subproblem as CCG subproblem.

3.3.1 NCCG Master Problem

In this section, we formulate the master problem for nested column-and-constraint generation algorithm.

Given a subset of worst-case attack plans $\hat{\mathbf{V}} = \{\hat{\mathbf{v}}^1, \ldots, \hat{\mathbf{v}}^k\} \subseteq \mathbb{V}$, we construct and solve the out level Master Problem to obtain a feasible protection plan. Note that, for a particular

attack plan $\hat{\mathbf{v}}^i$ ($\hat{\mathbf{v}}^i = \{\hat{v}_l^i, \forall l \in \mathbf{L}\}$), we define a set of dispatch variables $(\mathbf{p}^i, \mathbf{g}^i, \mathbf{d}^i, \boldsymbol{\delta}^k)$ that are associated with this particular attack plan. Then, the out level Master Problem can be constructed as follows.

$$\min \ \ \alpha \tag{3.11}$$

$$st. \ \alpha \geqslant \sum_{n \in \mathbf{N}} d_n^i, \ \ \forall i = 1, ..., k \tag{3.12}$$

$$\sum_{l \in \mathbf{L}} z_l \leqslant R \tag{3.13}$$

$$p_l^i x_l = {w_l}^i (z_l + {\hat{v}_l}^i - z_l {\hat{v}_l}^i)[\delta_{o(l)}^i - \delta_{d(l)}^i], \forall l \in \mathbf{L}, \forall i = 1, ..., k \tag{3.14}$$

$$\sum_{j \in \mathbf{Jn}} g_j^i - \sum_{l|o(l)=n} p_l^i + \sum_{l|d(l)=n} p_l^i + d_n^i = D_n, \forall n \in \mathbf{N}, \forall i = 1, ..., k \tag{3.15}$$

$$-P_l \leqslant p_l^i \leqslant P_l, \ \ \forall l \in \mathbf{L}, \forall i = 1, ..., k \tag{3.16}$$

$$0 \leqslant g_j^i \leqslant G_j, \ \ \forall j \in \mathbf{J}, \forall i = 1, ..., k \tag{3.17}$$

$$0 \leqslant d_n^i \leqslant D_n, \ \ \forall n \in \mathbf{N}, \forall i = 1, ..., k \tag{3.18}$$

$$z_l \in \{0, 1\}, \ \ \forall l \in \mathbf{L}. \tag{3.19}$$

To linearize (3.14), we replace it with following constraints.

$$0 \leqslant r_l^i \leqslant 1, \ \ \forall l \in \mathbf{L}, \forall i = 1, ..., k \tag{3.20}$$

$$r_l^i \leqslant w_l^i, \ \ \forall l \in \mathbf{L}, \forall i = 1, ..., k \tag{3.21}$$

$$r_l^i \leqslant z_l + {\hat{v}_l}^i - z_l {\hat{v}_l}^i, \ \ \forall l \in \mathbf{L}, \forall i = 1, ..., k \tag{3.22}$$

$$r_l^i \geqslant (z_l + {\hat{v}_l}^i - z_l {\hat{v}_l}^i) + w_l^i - 1, \ \ \forall l \in \mathbf{L}, \forall i = 1, ..., k \tag{3.23}$$

$$p_l^i x_l - [\delta_{o(l)}^i - \delta_{d(l)}^i] \leqslant M_p(1 - r_l^i), \forall l \in \mathbf{L}, i = 1, ..., k \tag{3.24}$$

$$p_l^i x_l - [\delta_{o(l)}^i - \delta_{d(l)}^i] \geqslant M_p(r_l^i - 1), \forall l \in \mathbf{L}, i = 1, ..., k \tag{3.25}$$

$$-P_l r_l^i \leqslant p_l^i \leqslant r_l^i P_l, \ \ \forall l \in \mathbf{L}, \forall i = 1, ..., k. \tag{3.26}$$

Since $\hat{\mathbf{V}} = \{\hat{\mathbf{v}}^1, \ldots, \hat{\mathbf{v}}^k\}$ is a subset of all possible attack plans, the out level Master Problem is a relaxation of the original model. As a relaxation of the original problem, the out level master problem provides a lower bound.

3.3.2 NCCG Subproblem

Solving the NCCG master problem will also give a feasible protection plan. We formulate the NCCG subproblem to obtain a feasible solution and an upper bound. Given hardening plan $\hat{\mathbf{z}}$, $\hat{\mathbf{z}} = \{\hat{z}_l, \forall l \in \mathbf{L}\}$, the NCCG subproblem can be formulated as follows.

$$\max_{\mathbf{v} \in \mathbb{V}} \min_{\mathbf{w} \in \mathbb{W}} \sum_{n \in \mathbf{N}} d_n \tag{3.27}$$

$$st. \ p_l x_l - w_l(\hat{z}_l + v_l - \hat{z}_l v_l)[\delta_{o(l)} - \delta_{d(l)}] = 0, \ \ \forall l \in \mathbf{L} \tag{3.28}$$

$$\sum_{l \in \mathbf{L}} (1 - v_l) \leqslant K \tag{3.29}$$

$$-P_l \leqslant p_l \leqslant P_l, \ \ \forall l \in \mathbf{L} \tag{3.30}$$

$$\sum_{j \in \mathbf{Jn}} g_j - \sum_{l|o(l)=n} p_l + \sum_{l|d(l)=n} p_l + d_n = D_n, \forall n \in \mathbf{N} \tag{3.31}$$

$$0 \leqslant g_j \leqslant G_j, \ \ \forall j \in \mathbf{J} \tag{3.32}$$

$$0 \leqslant d_n \leqslant D_n, \ \ \forall n \in \mathbf{N} \tag{3.33}$$

$$v_l, w_l \in \{0, 1\}, \ \ \forall l \in \mathbf{L}. \tag{3.34}$$

Given a protection plan $\hat{\mathbf{z}}$ (a solution from NCCG master problem), and a set of transmission line switching plans $\hat{\mathbb{W}} = \{\hat{\mathbf{w}}^s, s = 1, ..., t\}$ (solutions from CCG subproblems, t is the current iteration number of column-and-constraint generation loop), CCG master problem can be formulated as follows.

$$\max_{\mathbf{v}\in\mathbb{V}} \quad \beta \tag{3.35}$$

$$s.t.\ \ \beta \leqslant \sum_{n} D_n(\pi_n^{2^s} - \pi_n^{6^s}) - \sum_{j} G_j \pi_j^{3^s} - \sum_{l} P_l(\pi_l^{4^s} + \pi_l^{5^s}),\ \ \forall s = 1, ..., t \tag{3.36}$$

$$\sum_{l\in\mathbf{L}} (1 - v_l) \leqslant K \tag{3.37}$$

$$x_l \pi_l^{1^s} - \pi^{2^s}{}_{n,o(l)=n} + \pi^{2^s}{}_{n,d(l)=n} + \pi_l^{4^s} - \pi_l^{5^s} = 0,\ \ \forall l \in \mathbf{L}, s = 1, ..., t \tag{3.38}$$

$$\pi^{2^s}{}_{n,j\in Jn} - \pi_j^{3^s} \leqslant 0, \forall j \in \mathbf{J}, s = 1, ..., t \tag{3.39}$$

$$\pi_n^{2^s} - \pi_n^{6^s} \leqslant 1,\ \ \forall n \in \mathbf{N}, s = 1, ..., t \tag{3.40}$$

$$- \sum_{l,o(l)=n} \pi_l^{1^s} \hat{w_l}^s (\hat{z}_l + v_l - \hat{z}_l v_l) + \sum_{l,d(l)=n} \pi_l^{1^s} \hat{w_l}^s (\hat{z}_l + v_l - \hat{z}_l v_l) = 0,$$

$$\forall n \in \mathbf{N}, s = 1, ..., t \tag{3.41}$$

$$\pi_l^{1^s} free, \pi_l^{4^s} \geqslant 0, \pi_l^{5^s} \geqslant 0,\ \ \forall l \in \mathbf{L}, s = 1, ..., t \tag{3.42}$$

$$\pi_n^{2^s} free, \pi_n^{6^s} \geqslant 0,\ \ \forall n \in \mathbf{N}, s = 1, ..., t \tag{3.43}$$

$$\pi_j^{3^s} \geqslant 0,\ \ \forall j \in \mathbf{J}, s = 1, ..., t \tag{3.44}$$

$$v_l \in \{0, 1\},\ \ \forall l \in \mathbf{L}. \tag{3.45}$$

Note that the nonlinear constraints in (3.41) cab be easily linearized using the big-M method. Given a protection plan $\hat{\mathbf{z}}$ (i.e., a solution from NCCG master problem), and an

attack plan $\hat{\mathbf{v}}$ (i.e., a solution from CCG master problem), the CCG subproblem can be formulated as follows.

$$\min_{\mathbf{w}} \sum_{n \in \mathbf{N}} d_n \tag{3.46}$$

$$st.\ p_l x_l = (\hat{z}_l + \hat{v}_l - \hat{z}_l \hat{v}_l) w_l [\delta_{o(l)} - \delta_{d(l)}],\ \ \forall l \tag{3.47}$$

$$\sum_{j \in \mathbf{Jn}} g_j - \sum_{l|o(l)=n} p_l + \sum_{l|d(l)=n} p_l + d_n = D_n, \forall n \in \mathbf{N} \tag{3.48}$$

$$-P_l \leqslant p_l \leqslant P_l,\ \ \forall l \in \mathbf{L} \tag{3.49}$$

$$0 \leqslant g_j \leqslant G_j,\ \ \forall j \in \mathbf{J} \tag{3.50}$$

$$0 \leqslant d_n \leqslant D_n,\ \ \forall n \in \mathbf{N} \tag{3.51}$$

$$w_l \in \{0, 1\},\ \ \forall l \in \mathbf{L}. \tag{3.52}$$

3.3.3 Algorithm Implementation

Next, we present the implementation steps of nested column-and-constraint generation algorithm as in Algorithm 2. $\hat{\mathbb{V}}$ is a subset of attack plans $\hat{\mathbb{V}} = \{\hat{\mathbf{v}}^1, \ldots, \hat{\mathbf{v}}^k\} \subseteq \mathbb{V}$ for NCCG master problem, $\hat{\mathbb{W}}$ is a subset of transmission switching plans $\hat{\mathbb{W}} = \{\hat{\mathbf{w}}^1, \ldots, \hat{\mathbf{w}}^s\} \subseteq \mathbb{W}$ for CCG master problem. The optimality tolerance gap of algorithm is ϵ.

A flowchart of the complete implementation of nested column-and-constraint generation algorithm is presented in Figure 6. Two loops of CCG based decomposition algorithm is demonstrated. As NCCG master problem, CCG master and sub problems, after linearization, are linear mixed-integer programs, they can be readily solved by professional mixed-integer programming solvers. We note that results in Intersection Theorem can help

Algorithm 2 : Nested column-and-constraint generation for DAD-TLS

Initialization: set $LB \leftarrow -\infty$, $UB \leftarrow \infty$, $\hat{\mathbb{V}} \leftarrow \varnothing$, iteration index $k \leftarrow 1$
while gap $\geqslant \epsilon$ **do**
    solve NCCG master problem, update LB with optimal value $objMP$, update protection plan $\hat{\mathbf{z}}$, and gap
    solve NCCG sub problem with protection plan $\hat{\mathbf{z}}$ by the **Subroutine** below, obtain objective value $objSP$ and attack plan $\mathbf{v}^*$, $UB \leftarrow min\{UB, objSP\}$, update gap and $k \leftarrow k+1$
    add $\mathbf{v}^*$ to $\hat{\mathbb{V}}$, create dispatch variables $(\mathbf{p}^k, \mathbf{g}^k, \mathbf{d}^k, \boldsymbol{\delta}^k)$, and add these variables (columns) with corresponding constraints to NCCG master problem
end while
return $\mathbf{z}^* \leftarrow \hat{\mathbf{z}}$ ■

Subroutine : Solving NCCG sub problem

Initialization: set $LB_{in} \leftarrow -\infty$, $UB_{in} \leftarrow \infty$, $\hat{\mathbb{W}} \leftarrow \varnothing$, and inner iteration index $s \leftarrow 1$
while $gap^{'} \geqslant \epsilon$ **do**
    solve CCG master problem, update UB_{in} with optimal objective value $objMP_{in}$, obtain attack plan $\hat{\mathbf{v}}$, $gap^{'}$
    solve CCG sub problem with attack plan $\hat{\mathbf{v}}$, obtain optimal value $objSP_{in}$ and an optimal transmission line switching plan $\hat{\mathbf{w}}^s$, update $LB_{in} \leftarrow min\{LB_{in}, objSP_{in}\}$, $s \leftarrow s+1$, $gap^{'}$
    add $\hat{\mathbf{w}}^s$ to $\hat{\mathbb{W}}$, create dual variables $(\pi^{1s}, \ldots, \pi^{6s})$, and add these variables(columns) and their corresponding constraints to CCG master problem
end while
return $\mathbf{v}^* \leftarrow \hat{\mathbf{v}}$

to reduce the solution space and, therefore, the computational complexity. Specifically, we include the following constraints in the CCG master problem formulation (for a given protection plan $\hat{\mathbf{z}}$)

$$v_l = 1, \ \forall\, l \in \mathbf{L} \text{ s.t. } \hat{z}_l = 1.$$

The following constraints are also added to the NCCG master problem (for attack plans in $\hat{\mathbb{V}}$).

$$\sum_{l:\hat{v}_l=0} z_l \geqslant 1, \ \forall\, \hat{\mathbf{v}} \ \in \hat{\mathbb{V}}.$$

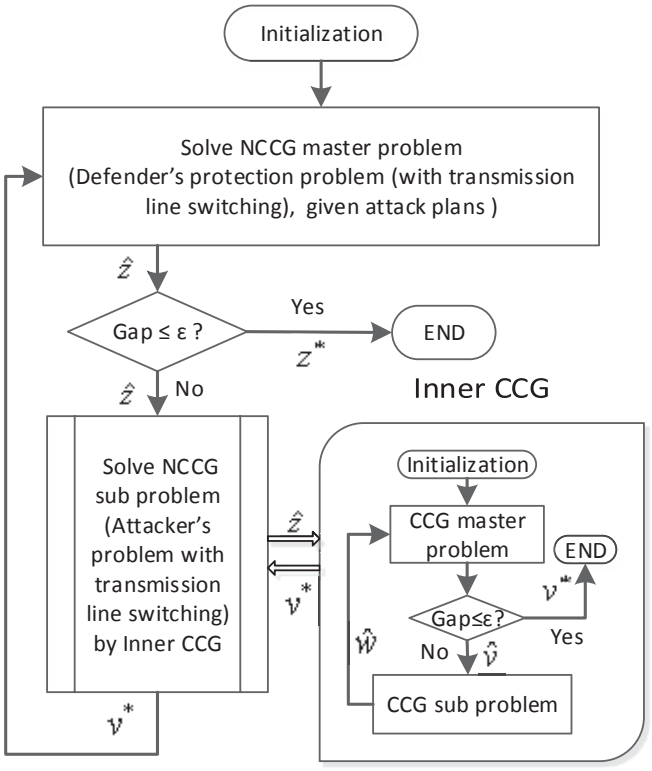

Figure 6: Flow chart of NCCG algorithm

3.4 Computational Studies

In this section, we conduct computational experiments on a well-known IEEE Reliability Test System (RTS) one-area (1996) [18]. This system consists of 24 buses, 38 lines, 32 generators and 17 loads as illustrated in Fig 7. Data and parameters are adopted from [5]. The algorithm is implemented in C++ with CPLEX 12.5 on top of an Intel dual core 3.00GHz, 4GB memory PC. Tolerance gap ϵ is 0.1%.

3.4.1 Computational Results

We first present the system total load shed and computational time with hardening budget R ranging from 0 to 4 and attack budget K ranging from 0 to 6. The load shed of optimal solutions are reported in Table 6 and their computational times are listed in Table 7.

N-K represents the worst-case contingency with K transmission lines under attack, specially, N-0 means no contingency in the grid.

Table 6: Load shed (MW) from DAD-TLS

N-K	$R = 0$	$R = 1$	$R = 2$	$R = 3$	$R = 4$
N-0	0	0	0	0	0
N-1	131	129	79	73	69
N-2	279	279	259	229	166
N-3	429	390	338	316	246
N-4	538	516	446	396	305
N-5	688	596	501	448	377
N-6	775	648	577	527	442

Table 7: Computational time (second) for DAD-TLS

N-K	$R = 0$	$R = 1$	$R = 2$	$R = 3$	$R = 4$
N-0	1.2	1.1	1.2	0.9	1.0
N-1	5.3	7.7	9.1	18.6	36.9
N-2	13.5	15.1	10.5	18.6	67.3
N-3	13.9	54.7	112	183	270
N-4	9.8	93.1	204	788	9268
N-5	4.6	328	20147	12365	42605
N-6	21.1	5116	71989	411123	111039

As expected, we observe in Table 6 that more protection budget R (or more attack budget K, respectively) leads to less (or more, respectively) load shed. Nevertheless, it can be seen that neither protection nor attack displays a linear behavior with respect to R or K in reducing or increasing the load shed, which indicates the complexity of physical laws and structures of a power grid. On the one hand, an empirical understanding is that a hardening plan with $R = 2$, if implemented in an optimal way, often leads to significant load shed reductions under different attack budgets. On the other hand, a similar understanding is that the worst N-2 contingencies could be very destructive.

In Table 7, we observe that for some instances the computation time could be very long, especially for those considering N-5 and N-6 contingencies, which can be explained by the combinatorial nature of DAD-TLS model. Because we are dealing with power grid long-term planning problem, which does not need to work in a real time fashion, such computational time could be addressed by adopting more powerful computing facilities with sufficient computational budgets. Another strategy is, according to Theorem 1, we can adopt optimal values from cases with N-K-1 and R-1 as strong bounds to facilitate the computation of those with N-K and R. Certainly, we will also explore advanced enhancement methods to improve the computational performance.

Indeed, due to the security or management issues in practice, we may not be able to switch off arbitrary transmission lines in the grid. Next, we study a few variants of DAD-TLS model where switching operations are restricted in different ways. For those variants, computational burdens are drastically reduced. To simplify our exposition, we refer to the original DAD-TLS with the full switching capability as DAD-OTS (optimal transmission switching).

3.4.2 A Few Variants of DAD-TLS

3.4.2.1 Budget for Transmission Line Switching

In practice, it is not practical to switch a large number of transmission lines when the power system is under attack. Consider the extreme case of transmission switching is all transmission lines are switched off. Hence, a power grid operator can put a budget on the number of switched transmission lines in respect of the system safety, which can be translated

into the following constraint to bound the total number of switching-offs in the inner most minimization problem,

$$\sum_{l \in L}(1 - w_l) \leqslant \text{PLS}$$

where PLS denotes the cardinality bound. The computational time and load shed results are listed in Table 8 and Table 9 with PLS = 4. Comparing the computational times in Table 9 with those in Table 7, we note that the computational time is greatly relieved by including a budget constraint on the total number of switched transmission lines. In the meantime, comparing results in Table 8 with those in Table 6, only 6 out of 35 cases incur slightly higher load shed. Those results suggest that we can achieve a trade-off between the load shed reduction and the computational time by assigning PLS to an appropriate value.

Table 8: Load shed (MW) from DAD-TLS with PLS=4

N-K	$R = 0$	$R = 1$	$R = 2$	$R = 3$	$R = 4$
N-0	00	0	0	0	0
N-1	135	129	105	73	69
N-2	279	279	264	229	179
N-3	429	390	346	316	246
N-4	538	516	446	396	321
N-5	688	596	501	448	377
N-6	775	648	577	527	442

Table 9: Computational time (second) for DAD-TLS with PLS=4

N-K	$R = 0$	$R = 1$	$R = 2$	$R = 3$	$R = 4$
N-0	1.2	0.7	1.0	1.0	0.8
N-1	2.4	3.7	6.7	12.3	28.1
N-2	2.9	3.2	5.1	22.3	124
N-3	9.5	20.5	20.2	103	139
N-4	9.4	14.3	60	170	5637
N-5	5.3	18.2	87.6	529	7297
N-6	7.7	29.5	158	484	971

3.4.2.2 Candidate Switchable Lines

In this part, we investigate one situation where only a proper subset of transmission lines are switchable. To achieve system stabilization, we may not want to switch off transmission lines that carry a significant amount of flow. So, we study one line switching strategy where only those with the least amount of power flows (measured when a power grid is in normal operating conditions: no attack/contingency) is switchable. In our experiment, we only allow the 10 least power flow lines to be switchable and computational results are reported in Table 10 and Table 11.

Table 10: Load shed (MW) of DAD-TLS

N-K	$R = 0$	$R = 1$	$R = 2$	$R = 3$	$R = 4$
N-0	110	110	110	110	110
N-1	197	190	190	172	171
N-2	307	279	278	277	251
N-3	429	411	366	338	316
N-4	538	516	446	402	396
N-5	688	596	501	473	466
N-6	775	648	575	553	525

Table 11: Computational time (second) of DAD-TLS

N-K	$R = 0$	$R = 1$	$R = 2$	$R = 3$	$R = 4$
N-0	0.4	0.3	0.3	0.2	0.3
N-1	0.6	1.2	1.4	3.2	3.3
N-2	1.1	2.4	2.5	3.6	12.6
N-3	2.1	3.2	4.3	12.6	30.0
N-4	3.5	4.0	8.2	47.5	49.4
N-5	4.1	8.2	35.0	55.5	65.1
N-6	6.0	11.3	40.0	146	192

Comparing results in Table 10 and Table 11 with those reported in previous tables, we note that the computational time is further drastically reduced. However, the performance in

reducing load shed is not satisfactory, especially for cases with $K \leqslant 3$. Such result indicates that only considering those transmission lines with the least flows as switchable is not very effective in mitigating contingencies. Other lines, which may carry a significant amount of power flow, could be more effective in post-contingency operations. A similar study is performed on a set of randomly selected transmission lines as switchable candidates. In Table 12 and 13, load shed and computational times of such candidate set with 10 randomly selected switchable candidate lines are reported. Similar to those in Table 10, the performance in reducing load shed is not satisfactory, which again confirms the challenge and the importance of selecting switchable candidates to mitigate contingencies.

Table 12: Load shed (MW) from DAD-TLS with candidate

N-K	$R = 0$	$R = 1$	$R = 2$	$R = 3$	$R = 4$
N-0	50	50	50	50	50
N-1	191	1.59	146	126	122
N-2	299	2.86	285	285	205
N-3	429	4.18	372	316	281
N-4	544	5.16	446	396	346
N-5	688	5.96	511	448	408
N-6	775	6.48	581	527	477

Table 13: Computational time (second) from DAD-TLS with candidate

N-K	$R = 0$	$R = 1$	$R = 2$	$R = 3$	$R = 4$
N-0	0.7	0.3	0.4	0.5	0.8
N-1	2.3	1.6	1.3	3.3	4.0
N-2	3.2	4.0	4.4	5.7	86.1
N-3	2.2	5.5	9.6	20.2	46.3
N-4	11.6	3.5	12.1	38.5	45.7
N-5	2.9	11.0	65.6	48.2	184.3
N-6	7.2	36.3	39.7	303	519.5

3.5 Benefit Analysis of Transmission Line Switching in Hardening

To investigate the benefits of incorporating transmission network topology control through optimal transmission line switching into power grid hardening problem, in this section, we make a comparison of the hardening plans derived from defender-attacker-defender model with optimal transmission line switching, i.e., DAD-OTS, and those obtained from traditional DAD model (without switching) [1].

3.5.1 Hardening Plans from Transmission Line Switching

We first demonstrate that with transmission line switching, an optimal protection plan derived from DAD-OTS model could be very different from that obtained from the classical DAD model. As shown in Figure 7 where $R = 2$ and $K = 2$, an optimal protection plan from DAD-OTS model consists of line 10-12 and line 12-23, while an optimal protection plan from DAD model consists of line 12-13 and line 20-23.

To have a complete benchmark, we present in Table 14 the total load shed of DAD model under all R and K combinations, which are derived in [1]. Comparing it with Table 6, we can confirm that load shed with transmission line switching is always less than those without transmission line switching. More straightforward comparisons can be found in Figure 8 and Figure 9, which present load shed (averaged over different hardening budgets) from DAD-OTS and DAD models under different N-K contingencies and the relative load shed reduction (in percentage) brought by transmission line switching.

As illustrated in Figures 8-9, transmission line switching has a very positive boosting effect on power grid hardening plans. In particular, for worst N-K contingencies with $K \leqslant 3$,

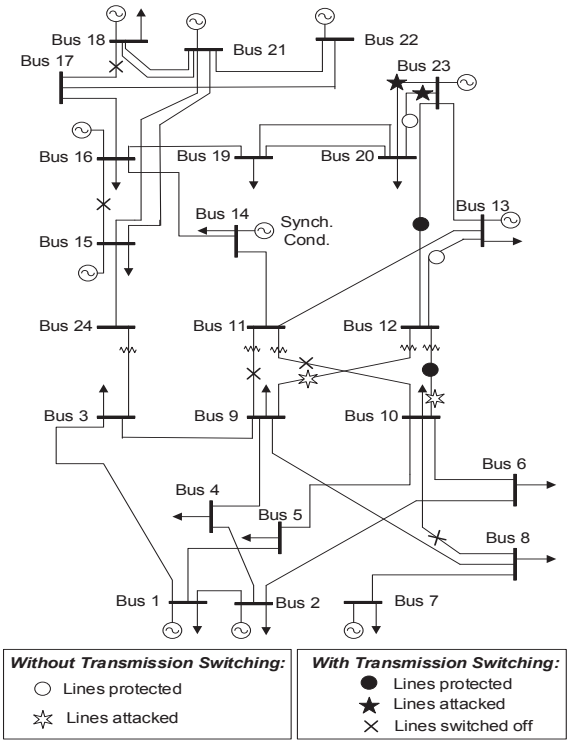

Figure 7: DAD-OTS and DAD solutions

more than 15% load shed reduction can be easily achieved, comparing to hardening plans generated from DAD model. Nevertheless, such effect reduces with respect to K. It can be explained by the fact that, with K getting larger, there is less switching freedom left among the survived transmission lines in the grid. Hence, the benefit of transmission line switching becomes smaller.

3.5.2 Cost-Effectiveness Analysis

With our developed computing methods for DAD-TLS and DAD models, we can investigate the minimum hardening budget (i.e., the least number of transmission lines for hardening) to achieve a desired level of load satisfaction under various N-K criteria, which therefore provides a basic cost-effectiveness analysis tool for hardening.

Table 14: Load shed (MW) from DAD model

N-K	$R = 0$	$R = 1$	$R = 2$	$R = 3$	$R = 4$
N-0	143	143	143	143	143
N-1	230	206	204	204	202
N-2	397	327	311	291	291
N-3	484	447	398	359	350
N-4	570	536	446	437	425
N-5	706	596	529	502	480
N-6	795	667	606	569	547

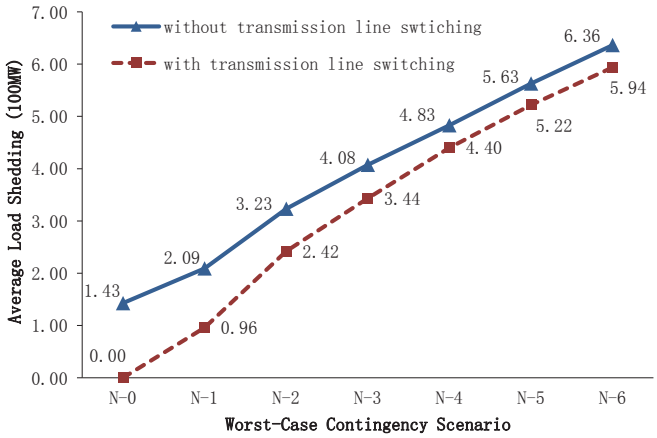

Figure 8: Load shed in different hardening plans

Next, we present a demonstration by considering the hardening budget under the worst N-3 contingency. A general understanding as shown in Figure 8 and Figure 9 is that with transmission switching, the load shed of a power grid considering N-3 contingency is always less than that of a power grid without transmission switching under various hardening budgets.

Figure 10 presents the numerical results between different load satisfaction requirements and protection budgets in DAD-OTS and DAD models. It is straightforward to realize that to have a higher proportion of load to be satisfied, we need larger protection budgets. However, hardening plans derived from DAD-OTS and DAD demand for drastically

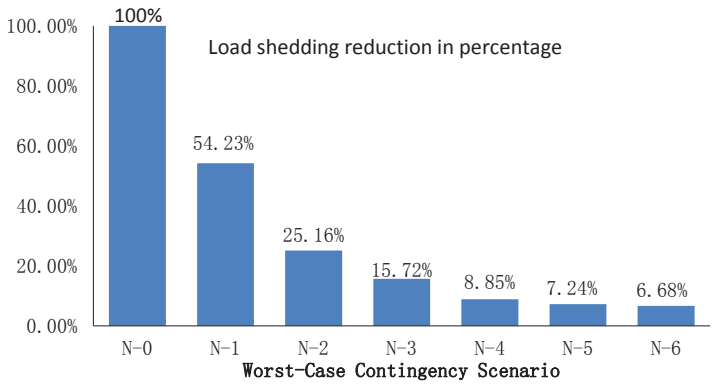

Figure 9: Load shed reduction in percentage

different economic investments. If we require that at least 85% total load must be met, 3 transmission lines should be hardened in the optimal DAD solution, while protecting 2 lines is sufficient in the optimal DAD-OTS solution. Such difference becomes more noticeable when the load satisfaction gets more stringent. For example, if at least 90% total load must be met, at least 14 lines should be hardened in optimal DAD solution while only 5 lines need to be protected in optimal DAD-OTS solution. Given the fact that practical transmission line hardening, e.g., placing lines underground, is very expensive, we can conclude that by modeling and implementing transmission line switching as a post-contingency operation, cost-effective protection plans can be derived that significantly outperform those obtained without considering this switching operation.

3.6 Conclusion

This chapter studies to incorporate transmission line switching operations into the traditional defender-attacker-defender model. For this challenging tri-level DAD-TLS formulation, we customize and implement nested column-and-constraint generation method to derive optimal solutions. A set of numerical experiments is performed on the IEEE one-area

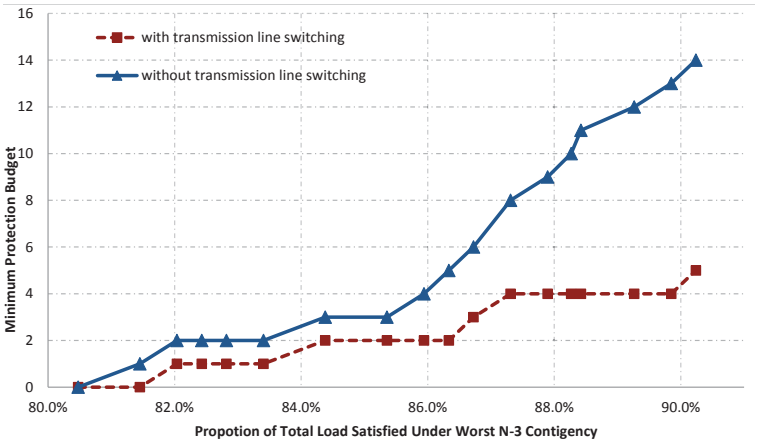

Figure 10: Hardening budget versus load satisfaction

RTS-96 system. Results verify the benefits of incorporating transmission line switching as a post-contingency operation into DAD model. In particular, it shows that resulting hardening plans from DAD-TLS could be different from those from DAD and they lead to very cost-effective hardening enhancement.

CHAPTER 4: ROBUST OPTIMIZATION BASED RESILIENT DISTRIBUTION NETWORK PLANNING AGAINST NATURAL DISASTERS

4.1 Introduction

Resilience of power grids against natural disasters has been a fundamental issue for the whole society. In recent years, hurricanes and extreme weather conditions have caused enormous economic losses and even human casualties. Since the mission of power industry is to keep the lights on, it is important to increase the resilience of existing power grids against the uncertain natural disasters. According to the report [19] prepared by the President's Council of Economic Advisers and the U.S. Department of Energy, power outages that occurred in the United States due to severe weather contributed to 58% of U.S. grid outages and cost the economy an annual average of 18 to 33 billion dollars between 2003 and 2012. Unfortunately, the impacts and financial costs of natural disasters related to floods, drought, and other weather events are expected to increase in significance as what are historically considered to be rare events are becoming more common and intense due to the climate change [33]. It is also emphasized that continued investment in grid modernization and resilience will mitigate these costs over time, saving the economy billions of dollars and reducing the hardship experienced by millions of Americans [19]. However, hardening and modernizing the whole grids is impossible due to its high cost. Hence, how to effectively

allocate budget limited resources to design a resilient power grid against natural disasters remains a great challenge. Due to the complex nature of this problem, various optimization models are proposed to facilitate the decision making process. These models range from mixed-integer programs and quadratic programs to more sophisticated stochastic programs and robust optimization to take account of the uncertainties involved.

4.1.1 Literature Review

As emphasized in [19], hardening is considered to be one of the most effective approaches that can increase the resilience of a power grid through undergrounding power lines, vegetation management, pole reinforcing, stockpiling power lines, etc. Previous research on power grid hardening planning [1, 11, 12, 22, 34] focuses on the hardening of transmission networks considering the uncertainty of terrorist attacks or natural disasters. The uncertain terrorist attack or natural disaster models are often formulated as an $N-K$ worst-case network interdiction problem [10, 32]. However, the static budget uncertainty set in this model ignores the spatial and temporal dynamics of the occurrence of a natural disaster. The hardening planning problem on transmission systems is generally formulated as a defender-attacker-defender sequential game model, which is equivalent to a two-stage robust optimization problem. Heuristics and exact solutions are proposed to solve the complicated tri-level program. In fact, the optimal solution of the model guarantees the effectiveness of hardening under the worst-case attack by alleviating system damage.

However, much less work has been done in recent years to support the hardening planning on distribution networks although storm-related outages often occur on distribution

systems. In fact, about 90% of outages during the storm event occur on distribution systems [19]. The models for hardening transmission networks are not directly applicable to hardening distribution networks because distribution networks mostly possess a radial tree-like network topology while transmission networks are more connected meshed networks. The relatively simple linear program based DC power flow models, which ignore reactive power and voltage profiles, are widely used in transmission networks to approximate the power flow. However, distribution networks require the consideration of reactive power and voltage profiles in the power flow calculation as demonstrated in [35].

In [36], a two-stage stochastic mixed-integer program for designing a resilient distribution network against natural disaster is presented, where damage scenarios from natural disasters are modeled as a set of stochastic events. A multi-commodity network flow model is used to approximate the power flow in the distribution network. The stochastic events on a distribution network are predetermined with certain components at fault. A two-stage robust optimization model for the distribution network reconfiguration considering load uncertainty is proposed in [37]. A mitigation method for electric distribution networks after natural disasters by sectionalizing a distribution network into microgrids with distributed generation (DG) units is presented in [38].

In the meantime, distributed generation resources impact critically the operations of a distribution system. DG can improve power quality, enhance the reliability of supply, and reduce system losses [39, 40]. The DG placement problem has therefore attracted the interest of many research efforts in the last two decades since it can provide the distribution system

operators, regulators and policy makers useful input for the derivation of incentives and regulatory measures. A common use of DG is serving as generation backup in case of main supply interruption [39] or natural disasters [38]. In [41], a robust optimization based model is proposed for placing DG units in microgrids with the consideration of load uncertainty over the planning horizon. It is meaningful to plan the investment of DG units in view of uncertain natural disasters since one of the main purposes of DG is to backup the system during natural disasters.

4.1.2 Our Approach

This paper proposes a robust optimization based decision support tool for the planning of a resilient distribution network. The optimal solution provides a network planning decision that coordinates the hardening and DG resource placement and improves the resilience of the distribution system against natural disasters.

The key contributions of the paper include are the following. First of all, we extend the traditional attacker-defender game based $N-K$ worst-case network interdiction model to a more practical multi-stage network interdiction model with a multi-stage and multi-zone based uncertainty set to capture the spatial and temporal dynamics of natural disasters such as hurricanes. Secondly, a robust optimization based framework that considers uncertain natural disaster occurrence is proposed to coordinate the planning of distribution systems using hardening and DG resource placement. Thirdly, A computational algorithm is developed for solving the model. The empirical studies validate the effectiveness of the proposed model. Last but not least, results reveal the importance of DG, which transforms a distribu-

tion network into several microgrids, in improving the distribution system's resilience under natural disasters.

The remainder of the chapter is organized as follows. Section 4.2 describes the modeling of network planning decisions, natural disaster modeling, power flow model and two-stage robust optimization formulation. Section 4.3 provides the column-and-constraint based decomposition algorithm for the model. Section 4.4 presents the empirical results and discusses the effectiveness of the proposed model. Finally, a conclusion and discussion about future research is given in Section 4.5.

4.2 Mathematical Formulation

In this section, we will present the planning decision set that coordinates hardening and DG resource placement, the modeling of natural disaster occurrence, the power flow model for the distribution network and the two-stage robust optimization model for the overall distribution network planning problem.

4.2.1 Network Planning Decisions

With a limited budget, a utility makes a plan to allocate budget limited resources in order to enhance the resilience of a distribution system. In this paper, we consider hardening power lines and DG resource placement. Other measures can be accommodated by reformulating the planning decision set accordingly.

Hardening is a preventive measure that will increase the resilience of a power grid under malicious terrorist attacks or natural disasters [19]. It is assumed that the hardened lines will survive the disasters [1, 11, 12, 34, 42]. Here we use a cardinality budget set similar to

Table 15: Nomenclature used in Chapter 4

$\mathbf{N}$	set of indices of nodes
$\mathbf{L}$	set of indices of branches, i.e., power lines
$\mathbf{T}$	set of indices of time periods
n	node index, $n \in \mathbf{N}$
(i, j)	power line from node i to node j, directed, $(i, j) \in \mathbf{L}$
t	time period index, $t \in \mathbf{T}$
Z_t	set of power lines affected in Zone t
$\mathbb{U}$	natural disaster uncertainty set
$\mathbb{Y}$	network planning decision set
$\mathbb{F}(\mathbf{h}, \mathbf{u})$	feasible set of power flow given $\mathbf{h}, \mathbf{u}$
H	budget for hardening power lines
G	budget for installing distributed generation units
C_d	monetary planning budget
x_{ij}, r_{ij}	reactance and resistance of power line (i, j)
P_{nt}, Q_{nt}	active and reactive power demand at node n in period t
G_n^p	capacity of distributed generation unit n
$\underline{v}, \overline{v}$	lower and upper bounds on voltage levels
y_{ij}	binary, 1 if line (i, j) is hardened, 0 otherwise
δ_n	binary, 1 if a distributed generator is placed at node n, 0 otherwise
$u_{ij,t}$	binary, 0 if power line (i, j) is damaged during a natural disaster in period t, 1 otherwise
v_{nt}	voltage magnitude at node n in period t
g_{nt}^p	active power generation of the distributed generation unit at node n in period t
g_{nt}^q	reactive power supply at node n in period t.
$p_{ij,t}, q_{ij,t}$	active and reactive power flow on power line (i, j) in period t
p_{nt}^{ld}	load shed at node n in period t
$\mathbf{p}, \mathbf{q}, \mathbf{v}$	vectors of active power variables $p_{ij,t}$, reactive power variables $q_{ij,t}$, and voltage variables v_{nt}
$\mathbf{h}$	concatenation of vector y_{ij} and vector δ_n, a network planning scenario
$\mathbf{u}$	vector of $u_{ij,t}$, a natural disaster scenario
$\mathbf{z}$	vector of power flow variables including active power flow, reactive power flow, and voltage levels

the budget sets used in hardening transmission networks [1, 11, 34, 42]. Additionally, DG has been gaining interests as an effective tool for reliability, losses and voltage improvements [40], and also as a reliable energy source that can start almost instantaneously when a major contingency occurs in a distribution system [43]. To study the effectiveness of DG on system resilience during natural disasters and analyze the optimal placement of DG resources, we assume that there is a cardinality budget for the available DG units. Hence, a budget set for the decision maker can be formulated as follows.

$$\mathbb{Y} = \left\{ \sum_{(i,j)\in L} y_{ij} \leqslant H, \sum_{n\in N} \delta_n \leqslant G \right\}$$

This decision set assumes that the decision maker has a budget to harden a maximum of H power lines and to place a maximum of G DG units. As a matter of fact, we can easily modify the decision set to accommodate more sophisticated decision scenarios, such as considering the cost variations of DG units and hardening different power lines. A simple example similar to [12] is to consider the hardening cost to be proportional to the length of a power line. Thus, we specify a hardening cost c_l for each line and a cost c_n for each DG unit. Assuming that the total investment cannot exceed a monetary budget C_d, an alternative network planning decision set can be formulated as $\mathbb{Y}^{'}$.

$$\mathbb{Y}^{'} = \left\{ \sum_{(i,j)\in L} c_{ij} y_{ij} + \sum_{n\in N} c_n \delta_n \leqslant C_d \right\}$$

4.2.2 Natural Disaster Occurrence Model

Natural disasters are generally highly uncertain events that are difficult to predict, estimate and model. A lot of efforts are made to increase our awareness of natural disasters based on historical data and the lessons we learned. The forecasting of a natural disaster is often based on statistical models or simulation models as reviewed in [44]. Predefined natural disaster scenarios are assumed in [36] with uniform probability. In this paper, we develop a multi-stage natural disaster occurrence model based on the traditional $N - K$ network interdiction model to capture the spatial and temporal dynamics of a natural disaster. To be specific, we consider the case of hurricanes.

4.2.2.1 Spatial and Temporal Dynamics of Hurricanes

As revealed by the Hurricane Forecast Improvement Program [45], a hurricane often follows a path that consists of multiple periods and several associated geographic zones (see Fig. 11). Also, the wind speed of a hurricane, which is one of the most destructive forces of a hurricane, decreases once the storm lands and drifts away from the sustaining heat and moisture provided by ocean or gulf waters. This can be seen from Fig. 12 that wind speed quickly decays over time after landfall. Geographically, the wind speed decays along its path as shown in Fig. 13 based on the inland wind model [46].

4.2.2.2 Modeling Natural Disasters on Power Grids

Terrorist attacks or natural disaster occurrences on a power system are often modeled as an attacker-defender game, i.e., the bi-level worst-case network interdiction model as used in [1, 8, 10–12, 32, 34, 42], where the outer level represents the attacker's decision with limited

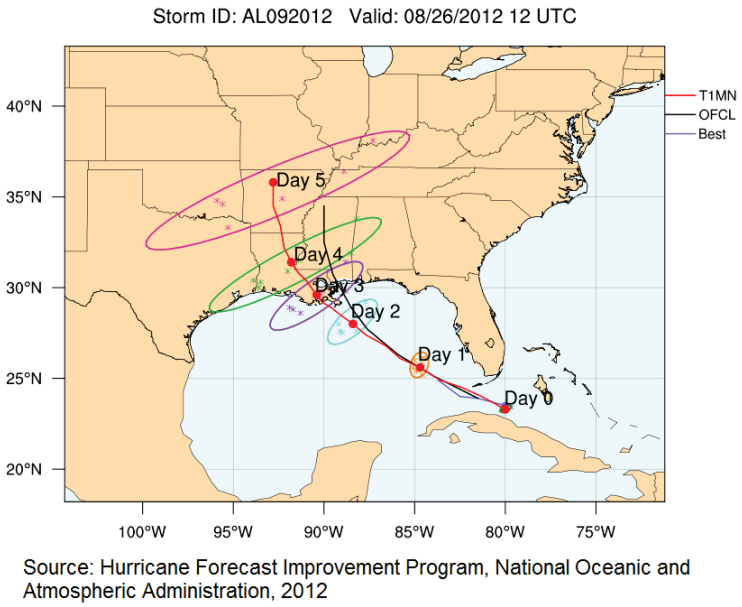

Figure 11: A typical evolution of hurricane

attack resources and the lower level is a defenders recourse decision with a re-dispatch of power flow based on the damage caused by the attacker. The attacker's decision set is defined by an uncertainty set with a limited budget of attack resources. This budget reflects the system operator's estimation of the damage level caused by possible attacks. As a matter of fact, uncertainty sets have been widely used in power systems to capture various uncertain factors, such as uncertain demand [47–50], renewable generation [51], system contingency [26, 52], terrorists attacks. and natural disasters [1, 8, 11], etc. In this study, we also use the attacker-defender game based network interdiction model to model the impacts of natural disasters since this approach gives the worst-case scenario of all feasible natural disaster scenarios in the feasible set of attacker. However, different from the traditional attacker-defender models [11, 14, 31, 32], where a simple cardinality budget constraint on the whole system damage is assumed, the uncertainty set in this paper takes account of the spatial

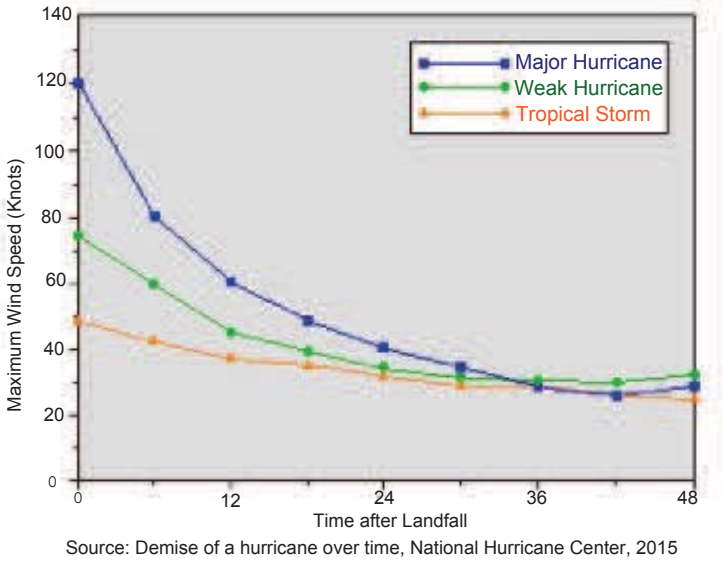

Figure 12: Decay of hurricane attack

and temporal dynamics of a natural disaster by constructing a more realistic uncertainty set as an extension to the traditional $N-K$ worst-case contingency based natural disaster model. Based on the spatial and temporal dynamics of a hurricane, we assume that when a hurricane moves into an area, it will land on the zone that is close to the coastline and the flood and strong rotating wind will impact the power lines within the zone whereas the far-away power lines will stay intact. Within the affected zone, an $N-K$ contingency network interdiction model is used to estimate impacts of the hurricane. As the hurricane pushes towards the inland area, it will affect the regions from one zone to another based on the geographic locations.

An illustrative case based on the IEEE 33-node distribution system is provided in Fig. 14. First of all, the distribution system is divided into several zones based on the path of the hurricane movement and the geographic locations of the power lines. Zone 1 is close

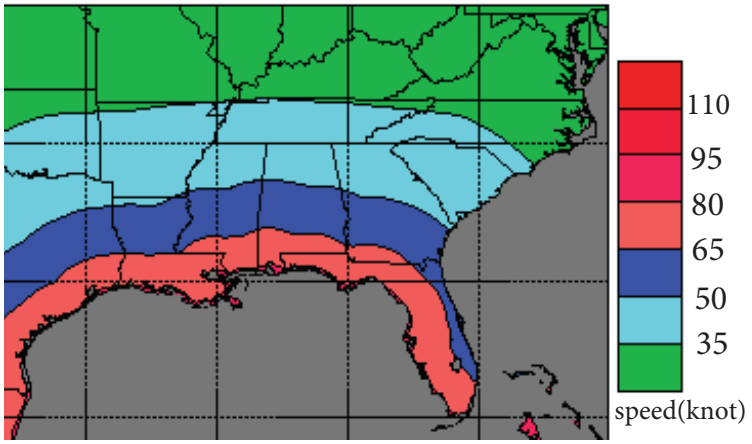

Source: The inland wind model, National Hurricane Center, 2015

Figure 13: Extent of inland winds from category 3 hurricanes

to the coastline, which will suffer from the hurricane impact first. In the second period, the hurricane will move to the inland area and cause damage to the power lines in Zone 2. Finally, the hurricane will reach Zone 3. Hence, we can divide the hurricane occurrence into multiple periods and zones based on the path of the hurricane. This type of natural disaster event can be described using the flowing uncertainty set $\mathbb{U}$.

$$\mathbb{U} = \left\{ \begin{array}{l} \sum\limits_{(i,j)\in Z_1} (1-u_{ij,1}) \leqslant B_1, \\ u_{ij,1} = 1, \forall (i,j) \in \mathbf{L} \backslash Z_1, \\ \sum\limits_{(i,j)\in Z_2} (1-u_{ij,2}) \leqslant B_2, \\ u_{ij,2} = u_{ij,t-1}, \forall (i,j) \in \mathbf{L} \backslash Z_2, \\ ..... \\ \sum\limits_{(i,j)\in Z_T} (1-u_{ij,T}) \leqslant B_T, \\ u_{ij,t} = u_{ij,t-1}, \forall (i,j) \in \mathbf{L} \backslash Z_t, t = T, \end{array} \right\}$$

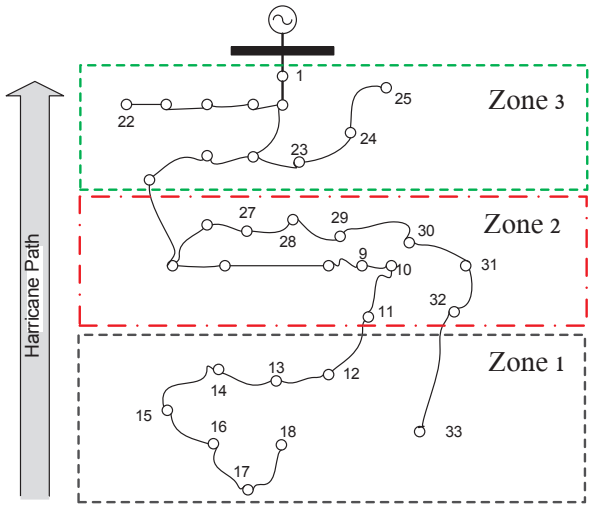

Figure 14: A hurricane occurrence model

where B_t is the cardinality budget for the number of damaged lines in the affected zone Z_t for period t. Constraints $u_{ij,t} = u_{ij,t-1}, \forall (i,j) \in \mathbf{L} \backslash Z_t$ mean that the power lines not in the affected zone of period t will remain the same as their previous status. In this method, the hurricane impact within each zone is formulated as an $N-K$ worst-case network interdiction problem. The uncertainty set becomes the traditional $N-K$ worst-case contingency analysis if the whole distribution system is considered as one zone that is affected at the same time. The above uncertainty set describes the feasible set of the attacker in the attack-defender model. The operational power flow model for the defender is presented in the following distribution network power flow model.

4.2.3 Distribution Network Power Flow

4.2.3.1 DG Operations

When a natural disaster occurs to a distribution system, backup or standby DG units such as fossil fueled combustion generators will pick up certain lost load. A previous paper

[41] on DG placement assumes that if a DG unit is placed at node n, this DG unit can supply power to node n and the child branches of node n in the radial tree network, where the substation is regarded as the root node of the tree. No power flow is allowed form node n to its parent node. Even though system reconfiguration, through which a power system still maintains a radial topology [35] or forms islanded microgrids [38], allows a DG to even serve its parent nodes in the original tree network, these techniques are not considered in this research. In fact, during or after a natural disaster occurrence, it is difficult for the distribution system operator to obtain the global information of the switch devices and other system status information through either the communication system or dispatched maintenance personnel, not to mention deploying a reconfiguration plan or remotely controlling switch devices with massive damage in the system. Hence, similar to [41], this paper assumes that a DG can supply power to the node it is placed and its child branches that are not damaged by the disaster attack.

4.2.3.2 Distribution Network Power Flow Model

The power flow model used in hardening transmission networks is often linear DC optimal power flow model [1, 8, 11] which considers active power and phase angles but ignores reactive power and voltage levels. Unlike the transmission systems, which are often meshed networks, the distribution networks mostly possess and maintain a tree-like radial topology. DistFlow [35] equations are often used to calculate the complex power flow and voltage profile in a distribution system [35, 38, 41, 53].

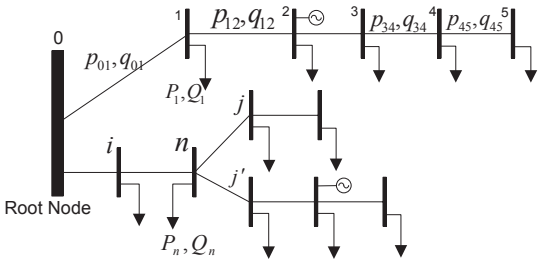

Figure 15: A typical radial distribution network

Based on [35], the DistFlow equations are defined as in equations (4.1) to (4.3). For simplicity, time index t is dropped in equations (4.1) to (4.6). For any node n, its parent node i, i.e., $(i, n) \in \mathbf{L}$, and its child nodes j, i.e., $(n, j) \in \mathbf{L}$.

$$\sum_{j|(n,j)\in\mathbf{L}} p_{nj} = p_{in} - r_{in}\frac{p_{in}^2 + q_{in}^2}{v_n^2} - P_n, \tag{4.1}$$

$$\sum_{j|(n,j)\in\mathbf{L}} q_{nj} = q_{in} - x_{in}\frac{p_{in}^2 + q_{in}^2}{v_n^2} - Q_n, \tag{4.2}$$

$$v_j^2 = v_i^2 - 2(r_{ij}p_{ij} + x_{ij}q_{ij}) + (r_{ij}^2 + x_{ij}^2)(\frac{p_i^2 + q_i^2}{v_i^2}),\ \forall(i,j) \in \mathbf{L}. \tag{4.3}$$

The linearized version of the power flow equations has been extensively justified and used in distribution systems [35, 38, 41, 53]. Considering the whole radial network, DG and load shed, equations (4.1) to (4.3) can be simplified as follows.

$$\sum_{j|(n,j)\in\mathbf{L}} p_{nj} = p_{in} - P_n + g_n^p + p_n^{ld}, \tag{4.4}$$

$$\sum_{j|(n,j)\in\mathbf{L}} q_{nj} = q_{in} - Q_n + g_n^q, \tag{4.5}$$

$$v_j = v_i - \frac{r_{ij}p_{ij} + x_{ij}q_{ij}}{V_0},\ \forall(i,j) \in \mathbf{L}. \tag{4.6}$$

To be specific, (4.4) and (4.5) represent that the active and reactive power flow are balanced at each node. (4.6) respects the voltage level at each node. In our model, the distribution network topology depends on network planning decisions and the uncertainty set of the natural disaster. This relationship can be described as follows.

$$0 \leqslant p_{ij,t} \leqslant M_t^1(y_{ij} + u_{ij,t}), \ \ \forall t \in \mathbf{T}, (i,j) \in \mathbf{L} \tag{4.7}$$

$$0 \leqslant q_{ij,t} \leqslant M_t^2(y_{ij} + u_{ij,t}), \ \ \forall t \in \mathbf{T}, (i,j) \in \mathbf{L} \tag{4.8}$$

$$0 \leqslant g_{nt}^p \leqslant \delta_n G_n^p, \ \ \forall t \in \mathbf{T}, n \in \mathbf{N} \tag{4.9}$$

(4.7) and (4.8) force the active and reactive power flow of a branch to be zero if the branch fails in the disaster ($u_{ij} = 0$) yet not hardened ($y_{ij} = 0$). However, if the branch is either hardened ($y_{ij} = 1$) or not damaged during attack ($u_{ij} = 1$), i.e., $u_{ij} + y_{ij} \geqslant 1$, the zero upper bound on p_{ij} and q_{ij} is removed. M_t^1 and M_t^2 are big M values. The easy values for M_t^1 and M_t^2 are the total active power demand and reactive power consumption in the distribution system respectively. Based on the above, the optimal power flow for distribution network after hardening and DG placement planning ($\mathbf{h}$) and disaster impact ($\mathbf{u}$) can be formulated as:

$$\mathbf{z} = (\mathbf{p}, \mathbf{q}, \mathbf{v}) \in \mathbb{F}(\mathbf{h}, \mathbf{u}) =$$

$$\{ \sum_{j|(n,j)\in\mathbf{L}} p_{nj,t} = p_{in,t} - P_{nt} + g_{nt}^p + p_{nt}^{ld}, \quad \forall t \in \mathbf{T}, n \in \mathbf{N}, (i,n) \in \mathbf{L} \tag{4.10}$$

$$\sum_{j|(n,j)\in\mathbf{L}} q_{nj,t} = q_{in,t} - Q_{nt} + g_{nt}^q, \quad \forall t \in \mathbf{T}, n \in \mathbf{N}, (i,n) \in \mathbf{L} \tag{4.11}$$

$$0 \leqslant g_{nt}^{p} \leqslant \delta_n G_n^p, \quad \forall t \in \mathbf{T}, n \in \mathbf{N} \tag{4.12}$$

$$0 \leqslant g_{nt}^{q} \leqslant Q_{nt}, \quad \forall t \in \mathbf{T}, n \in \mathbf{N} \tag{4.13}$$

$$0 \leqslant p_{nt}^{ld} \leqslant P_{nt}, \quad \forall t \in \mathbf{T}, n \in \mathbf{N} \tag{4.14}$$

$$\underline{v} \leqslant v_{n,t} \leqslant \overline{v}, \quad \forall t \in \mathbf{T}, n \in \mathbf{N} \tag{4.15}$$

$$0 \leqslant p_{ij,t} \leqslant M_t^1(y_{ij} + u_{ij,t}), \quad \forall t \in \mathbf{T}, (i,j) \in \mathbf{L} \tag{4.16}$$

$$0 \leqslant q_{ij,t} \leqslant M_t^2(y_{ij} + u_{ij,t}), \quad \forall t \in \mathbf{T}, (i,j) \in \mathbf{L} \tag{4.17}$$

$$v_{jt} = v_{it} - \frac{r_{ij}p_{ij,t} + x_{ij}q_{ij,t}}{V_0}, \quad \forall t \in \mathbf{T}, (i,j) \in \mathbf{L}\} \tag{4.18}$$

(4.12)-(4.13) restrain the active and reactive power generation at node n. (4.14) forces the upper bound of the unsatisfied real demand within its real demand. (4.15) ensures the voltage levels are within a predefined secure range. To simplify the notation, an abstract form of the above feasible set is given as:

$$\mathbb{F}(\mathbf{h}, \mathbf{u}) = \{\mathbf{z} : A\mathbf{h} + B\mathbf{u} + C\mathbf{z} \geqslant \mathbf{e}\}.$$

4.2.4 Robust Optimization Model

The overall resilient distribution network planning problem is formulated as a two-stage robust optimization problem [47, 50], which is also called a defender-attacker-defender game model [1, 11, 12, 22]. Even though the two-stage robust optimization and the defender-attacker-defender model may have different origins, they share an identical tri-level mathematical programming structure. The objective of the model is to minimize the unsatisfied

demand, i.e., load shed, in the distribution system over T periods under the worst-case natural disaster's attack. Feasible sets of $\mathbb{Y}$, $\mathbb{U}$, and $\mathbb{F}(\mathbf{h}, \mathbf{u})$ are defined as above.

$$\min_{\mathbf{h}\in\mathbb{Y}} \max_{\mathbf{u}\in\mathbb{U}} \min_{\mathbf{z}\in\mathbb{F}(\mathbf{h},\mathbf{u})} \sum_{n,t} p_{nt}^{ld} \tag{4.19}$$

4.3 Solution Methodology

In this section, we describe how to decompose the original model based on the column-and-constraint algorithm and formulate the corresponding master problem and subproblem for the proposed model (4.19).

4.3.1 CCG Master Problem

The CCG master problem contains a set of worst-case disaster scenarios $\hat{\mathbb{U}} = \{\hat{\mathbf{u}}^s, s = 1, 2, ..., k\}$. The worst-case disaster scenarios are obtained from the CCG subproblem over the iterations. Note that solving the CCG master problem yields a network planning decision $\hat{\mathbf{h}}$ and a lower bound of the original model since the CCG master problem is a relaxation of the original model. Indeed, if $\hat{\mathbb{U}}$ contains all possible disaster scenarios, the master problem is equivalent to the original model.

$$\min \alpha \tag{4.20}$$

$$st.\ \mathbf{h} \in \mathbb{Y} \tag{4.21}$$

$$\alpha \geqslant \sum_{n,t} p_{nt}^{ld,s}, \quad \forall s = 1, 2, ..., k \tag{4.22}$$

$$\mathbf{z}^s \in \mathbb{F}(\mathbf{h}, \hat{\mathbf{u}}^s), \quad \forall s = 1, 2, ..., k. \tag{4.23}$$

4.3.2 CCG Subproblem

The CCG subproblem seeks the worst-case natural disaster scenario with a given network planning decision $\hat{\mathbf{h}}$ from the CCG master problem. Let $\boldsymbol{\pi}$ be the vector of the dual variables for constraints (4.10)-(4.18) and $\boldsymbol{\Omega}_(\hat{\mathbf{h}}, \mathbf{u})$ denotes the feasible set of the dual inner linear program,

$$\boldsymbol{\Omega}_(\hat{\mathbf{h}}, \mathbf{u}) = \{\boldsymbol{\pi} : C^T \boldsymbol{\pi} \leqslant I\},$$

with a given hardening plan $\hat{\mathbf{h}}$. Then the bi-level subproblem can be transformed to a bilinear program as follows.

$$\begin{aligned} \max_{\mathbf{u}\in\mathbb{U}} \min_{\mathbf{z}\in\mathbb{F}(\hat{\mathbf{h}},\mathbf{u})} \sum_{n,t} p_{nt}^{ld} &= \max_{\mathbf{u}\in\mathbb{U}} \max_{\boldsymbol{\pi}\in\boldsymbol{\Omega}_(\hat{\mathbf{h}},\mathbf{u})} (\mathbf{e} - A\hat{\mathbf{h}} - B\mathbf{u})\boldsymbol{\pi} \\ &= \max_{\mathbf{u}\in\mathbb{U},\boldsymbol{\pi}\in\boldsymbol{\Omega}_(\hat{\mathbf{h}},\mathbf{u})} (\mathbf{e} - A\hat{\mathbf{h}} - B\mathbf{u})\boldsymbol{\pi} \end{aligned} \tag{4.24}$$

The above bilinear program can be linearized using the big-M method and then solved by an MIP solver. The solution from CCG subproblem together with the corresponding network planning solution $(\hat{\mathbf{h}}, \hat{\mathbf{u}}, \hat{\mathbf{z}})$ form a feasible solution for the original tri-level program and thus provide an upper bound for the original model.

4.3.3 Algorithm Implementation

The detailed algorithm implementation procedure is described in Algorithm 3. The tolerance gap of optimality for the algorithm is ϵ.

Algorithm 3 : CCG decomposition algorithm for RDNP

Initialization: set $LB \leftarrow -\infty$, $UB \leftarrow \infty$, $\hat{\mathbb{U}} \leftarrow \varnothing$, iteration index $k \leftarrow 0$, gap $\leftarrow \infty$, $\hat{\mathbf{h}} \leftarrow \mathbf{0}$
while gap $\geqslant \epsilon$ **do**
solve CCG subproblem with given plan $\hat{\mathbf{h}}$, obtain objective value $objSP$ and disaster scenario $\mathbf{u}^*$, $UB \leftarrow min\{UB, objSP\}$, update gap and $k \leftarrow k+1$;
add $\mathbf{u}^*$ to $\hat{\mathbb{U}}$, create dispatch variables ($\mathbf{z}^k$), and add these variables (i.e., columns) with corresponding constraints $\mathbf{z}^k \in \mathbb{F}(\mathbf{h}, \mathbf{u^k})$ to CCG master problem;
solve CCG master problem, update LB with optimal value $objMP$, update network planning plan $\hat{\mathbf{h}}$ and gap;
end while
return $\mathbf{h}^* \leftarrow \hat{\mathbf{h}}$. ■

4.4 Numerical Results

In this section, we perform computational experiments to test the proposed model and algorithm. The IEEE 33-node distribution network is used in this study. The parameters of the system are adopted from [35] with distributed generators initially located at nodes 7, 12, and 27, each with a capacity of 10 MW. The natural disaster occurrence model used is based on the uncertainty set $\mathbb{U}$ defined for hurricane attacks on the IEEE 33-node distribution system in Section II. The solution algorithm is implemented in C++ with CPLEX 12.6 on a dual-core PC with 6GB RAM.

4.4.1 Hurricane Occurrence

The optimal solution of the worst-case hurricane occurrence model is obtained by solving the bi-level attacker-defender model, i.e., CCG subproblem. As shown in Fig. 14, the whole dynamic evolution process of the hurricane is divided into three stages. During each period, the hurricane attack will cause power line failures with a cardinality budget. The power lines that failed in the previous time period will remain at fault in the next stage. Fig. 16 gives a worst case hurricane attack plan with the natural disaster uncertainty set

$(B_1 = 2, B_2 = 2, B_3 = 1)$, which means there are at most two power lines out for Zone 1 and Zone 2, and one power line out for Zone 3. The optimal solution of the hurricane occurrence model gives a worst-case hurricane scenario within a given uncertainty set. To be specific, in the first time period, lines 12-13 and 32-33 will be damaged as the hurricane lands in Zone 1. In the second period, the hurricane moves along its path and damages lines 7-8 and 27-28 in Zone 2. Finally, when the hurricane arrives in Zone 3, it cuts off line 1-2. This attack will cause a power outage of 5520 KW out of the total demand of 11435 KW. Note that this hurricane scenario dominates any other possible hurricane scenarios in the defined uncertainty set since it is the optimal solution of the attacker-defender model.

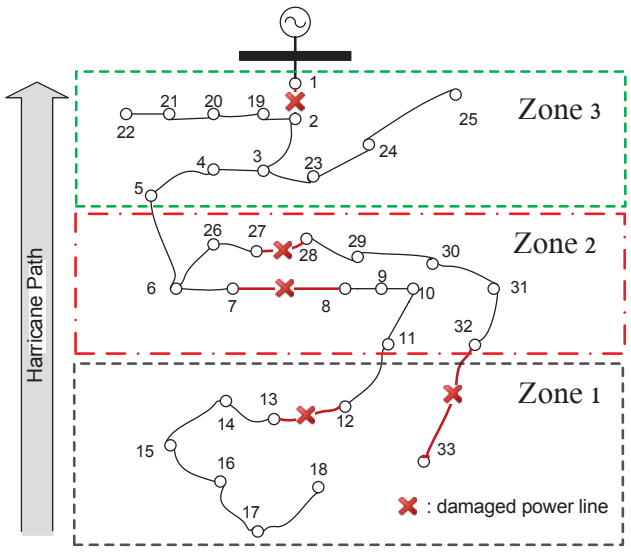

Figure 16: The worst-case hurricane scenario

4.4.2 Effectiveness of Hardening

To validate the effectiveness of hardening on distribution networks, we study the load shed in the distribution system under a hurricane scenario for various hardening budgets. The hurricane scenarios considered is $(B_1 = B_2 = B_3 = 1)$, which means that there will

be one uncertain power line damaged in the affected zone during each period. The optimal hardening plans, corresponding worst-case hurricane scenarios and load shed are given in Table 16 for hardening budget from $H = 0$ to $H = 6$. The power lines damaged under the worst-case hurricane scenarios are listed in the order of occurrence. Without hardening the system, this worst-case hurricane scenario will cause 4730 KW load shed in the grid. However, if we can harden one line (1-2), the load shed will be reduced to 4270 KW. Each time we add one more line to the hardening budget, the load shed for the uncertain natural disaster decreases. By hardening six power lines in the IEEE 33-node system, the load shed will be reduced from 4730 KW to 2830 KW, which is a reduction of more than 40%.

Table 16: Hardening plans

H	hardened lines	load shed (KW)	worst-case attack
0	None	4730	(12-13;27-28;1-2)
1	1-2	4270	(12-13;27-28;2-3)
2	1-2,2-3	3880	(12-13;27-28;3-23)
3	1-2,2-3,12-13	3700	(13-14;27-28;3-23)
4	1-2,2-3,12-13,13-14	3340	(12-13;6-26;3-23)
5	1-2,2-3,27-28,28-29,29-30	3120	(12-13;30-31;3-23)
6	1-2,2-3,12-13,13-14,3-23,23-24	2830	(14-15;27-28;24-25)

A more comprehensive study of the system load shed with different hardening budgets, $H = \{0, 1, ..., 33\}$ and different hurricane uncertainty sets, $(B_1 = B_2 = B_3 = 1)$, $(B_1 = B_2 = B_3 = 2)$, and $(B_1 = B_2 = B_3 = 3)$, is given in Fig. 17. As shown in Fig. 17, for all natural disaster occurrence scenarios, the load shed in the distribution system is monotonically decreasing with respect to the increase of the hardening budget. This proves the effectiveness of hardening. Moreover, for the same hardening budget, a stronger hurricane, i.e., a hurricane with larger B_1, B_2, and B_3, will cause more load shed in the system. In fact, this plot can

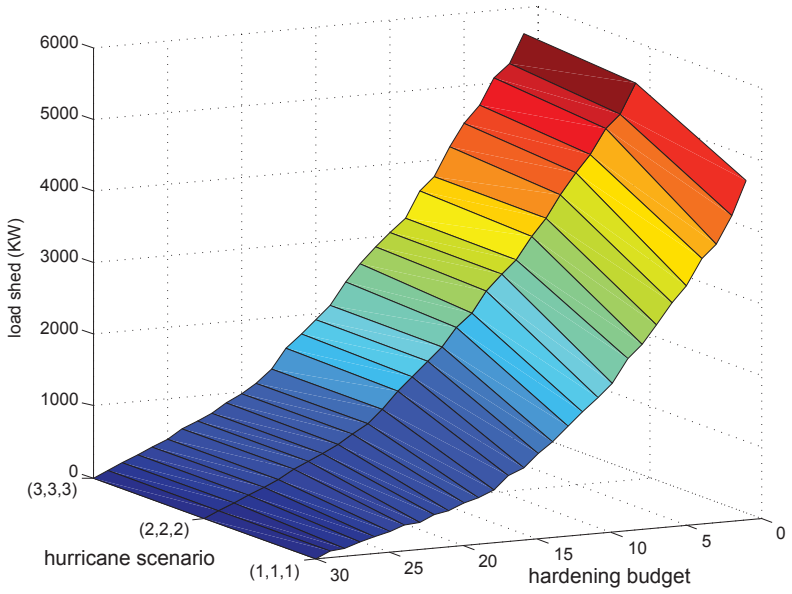

Figure 17: Load shed of distribution system

serve as a decision support tool to determine the hardening budget needed with respect to the estimated natural disaster category and the desired distribution system resilience level.

4.4.3 Influence of Distributed Generation

The DG units can continue supplying power to connected loads in the form of micro-grids when the distribution system is at fault [38, 43]. To investigate the importance of DG in the distribution system during natural disasters, a comparison among network planning without DG, with predefined DG and with optimal DG placement is studied. As can be seen from Fig. 18, the effectiveness of hardening in terms of reduced load shed in a hurricane is improved by DG as the load shed with DG is generally less than the case without DG, except for the case where every power line is hardened. Moreover, with a coordinated network planning solution of hardening and DG placement,i.e., the solution with optimal DG placement,

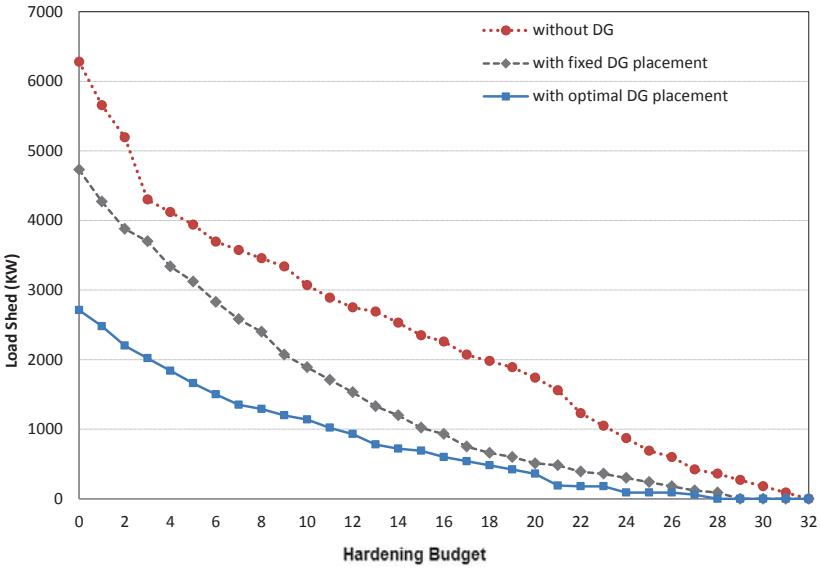

Figure 18: Impacts of DG on distribution system resilience

the distribution network is the most resilient among the three solutions as it results in the least load shed. In fact, when a distribution network is damaged by a natural disaster, the loads in branches that are disconnected from the main grid will be picked up by a DG unit if available. The DG units with connected branches will form microgrids where the power can be supplied by the DG within the microgrid. This interesting observation points to the importance of placing DG units and forming microgrids to increase the distribution network resilience under natural disasters as elaborated in [36, 38] and the necessity to coordinate the placement of DG resource placement with hardening in the distribution network planning process.

4.5 Conclusion

This chapter proposes a novel model for the planning of a resilient distribution system with hardening and distributed generation using two-stage robust optimization to minimize

the total load shed under natural disasters. The proposed model coordinates the optimal planning of hardening and DG resource placement. A multi-stage and multi-zone based uncertainty set is used to capture the uncertainty of natural disaster as an extension of the traditional $N-K$ interdiction model. A decomposition algorithm is designed and implemented to solve the tri-level program. Numerical results validate the effectiveness of model. Studies also point to the importance of placing distributed generation to increase the resilience of a distribution system against natural disasters.

CHAPTER 5: FAST DECOMPOSITION ALGORITHM FOR ROBUST UNIT COMMITMENT PROBLEM

5.1 Introduction

As one of the essential operation problems in power systems, unit commitment (UC) is an optimization problem that minimizes the system commitment cost and dispatch cost. Typically, such problem can be formulated as a mixed-integer program (MIP) model, including binary decisions on generators on/off status and continuous decisions on their generation levels and dispatch, subject to many physical restrictions and economic requirements, such as load balance constraints, transmission network constraints, generators' ramping up/down, min up/down time constraints, etc. Such MIP model is computationally sophisticated, noting that UC is an NP-hard problem [54] in nature.

Currently, the operations of large-scale power systems are facing increasing challenges from the penetration of renewable energy generation from the wind and solar, demand side management, smart grids, etc. These new technologies bring many nontrivial uncertainties and randomness into the operations of power grids and put the reliability of power system at risk. To handle those ubiquitous uncertainties in the system, various stochastic and robust UC models are developed and investigated. In particular, the robust UC has drawn intensive attentions from both academia and industry. One critical advantage it carries is that, instead of assuming alluring probability distribution for uncertain parameters in stochastic

Table 17: Nomenclature used in Chapter 5

j	generator index
l	transmission line index
n	bus index
t	time (hour) index
N	set of indices of buses
T	set of schedule horizon
J	set of indices of generators
Jn	set of indices of generators connected to bus n
L	set of indices of transmission lines
$o(l)$	origin bus of transmission asset l
$d(l)$	destination bus of transmission asset l
a_i	start up cost of unit i
c_i	fuel cost of unit i
c^{ls}	load shed penalty
c^{SU}_{jm}	start up cost of generator j for start up type m
$\underline{q}^{nt}$	lower bound of demand at bus n in time t
${}^{\triangle}q^{nt}$	uncertain part of demand at bus n in time t
P_l	power flow capacity of transmission line l
S_j	start-up segments of generator j
$\overline{\delta}$	phase angle capacity of connecting bus
DT_j	minimum down time of unit j
UT_j	minimum up time of unit j
$\overline{G}_j$	maximum output level of unit j
$\underline{G}_j$	minimum output level of unit j
RD_j	maximum ramp-down rate of unit j
RU_j	maximum ramp-up rate of unit j
SD_j	maximum shutdown rate of unit j
SU_j	maximum startup rate of unit j
T^{SU}_{jm}	offline hours of unit j
u_{jt}	binary, 1 if unit j is on in t, 0 otherwise
v_{jt}	binary, 1 if unit j is turned on at the start of t
w_{jt}	binary, 1 if unit j is turned off at the start of t
z_{nt}	binary, 1 if demand reaches upper bound in t, 0 otherwise
h_{jmt}	binary, startup-type m of unit j, which takes the value of 1 in the hour where units starts up and has been previously off-line within $[T^{SU}_{g,m}, T^{SU}_{g,m+1})$ hours
q_{nt}	power demand at bus n in time t
g_{jt}	power generation level of unit j in time t
d_{nt}	load shed at bus n in time t
δ_{nt}	phase angle at bus n in time t
p_{lt}	power flow on transmission line l in time t.

UC models, robust UC adopts a convenient uncertainty set to capture randomness and it guarantees that its solution, if derived, is feasible to any realization within the uncertainty set [50, 55, 56].

Though robust UC takes care of the uncertainties in determining UC decisions, the complexity of solving robust UC actually increases drastically, comparing with the basic UC model. Due to its complicated tri-level structure, directly computing robust UC using existing professional packages is not feasible. Instead, researchers and practitioners develop and implement two types of decomposition algorithms to solve it. One is based on classical Benders decomposition method [55–57]. The other one is a recent column-and-constraint generation [17] (CCG) method, which also employs a master-subproblem framework to exactly compute robust UC [50]. Comparing these two types of algorithms on both small-scale instances and large-scale ISO level power grids, it is observed that the CCG based solution procedure drastically outperforms the other one. We note that CCG method makes it possible to compute the day-ahead robust UC model on practical grids without considering transmission network constraints.

Nevertheless, in large grids, such as multi-state power grids that are managed by ISOs, we observe that the basic implementation of CCG method might not provide satisfactory computational performance. In particular, considering full network structures and their associated restrictions leads to heavy computational burdens on both the master and subproblems. To support real operations and practices in large grids, in this chapter, we study new computational improvement strategies for robust UC problem with the consideration of the

demand uncertainty. As a matter of fact, other types of uncertainties can be accommodated accordingly.

5.2 Problem Formulation

In this chapter, we consider the day-ahead unit commitment problem with J thermal units for T time periods for a power system with N buses and L transmission lines. In the remainder of this chapter, we follow the convention that one period stands for 60 minutes and thus T equals to 24 hours. Note that our model and solution method are applicable to any time scale. To minimize the operating cost and to meet physical requirements, generators' on/off status as well as start up operations need to be determined day-ahead while the actual generation outputs and market sell/buy decisions will be made in a real-time fashion. Hence, using the two-stage robust optimization modeling scheme, the robust unit commitment (RUC) problem is formulated as the following.

$$\min \sum_{t=1}^{T} \sum_{j \in J} (a_j u_{jt} + \sum_{m \in Sj} c_{jm}^{SU} h_{jmt}) + \max_{\mathbf{q} \in \mathbb{Q}} \min (\sum_{t=1}^{T} \sum_{j \in J} c_j g_{jt} + \sum_{t=1}^{T} \sum_{n \in N} c^{ls} d_{nt}) \tag{5.1}$$

$$s.t.\ h_{jmt} \leqslant \sum_{i=T_{jm}^{SU}}^{T_{j,m+1}^{SU}-1} w_{j,t-i},\ \ \forall j, t \in [T_{j,m+1}^{SU}, T] \tag{5.2}$$

$$\sum_{m \in S_j} h_{jmt} = v_{jt},\ \ \forall j, t \in [1, T] \tag{5.3}$$

$$\sum_{i=t-UT_j+1}^{t} v_{ji} \leqslant u_{jt},\ \forall j, t \in [UT_j + 1, T] \tag{5.4}$$

$$\sum_{i=t-DT_j+1}^{t} w_{ji} \leqslant 1 - u_{jt},\ \forall j, t \in [DT_j + 1, T] \tag{5.5}$$

$$u_{jt} - u_{j,t-1} = v_{jt} - w_{jt},\ \forall j, t \in [1, T] \tag{5.6}$$

$$g_{jt} - g_{j,t-1} \leqslant RU_j u_{j,t-1} + SU_j v_{jt},\ \forall j, t \in [1, T] \tag{5.7}$$

$$g_{j,t-1} - g_{j,t} \leqslant RD_j u_{jt} + SD_j w_{jt},\quad \forall j, t \in [1, T] \tag{5.8}$$

$$\underline{G} u_{j,t} \leqslant g_{jt} \leqslant \overline{G}_j u_{j,t},\ \ \forall j, t \in [1, T] \tag{5.9}$$

$$p_{lt} x_l = \delta_{o(l),t} - \delta_{d(l),t},\ \forall l \in \mathbf{L}, t \in [1, T] \tag{5.10}$$

$$\sum_{j \in \mathbf{Jn}} g_{jt} - \sum_{l|o(l)=n} p_{lt} + \sum_{l|d(l)=n} p_{lt} + d_{nt} = q_{nt},\ \forall n \in \mathbf{N}, t \in [1, T] \tag{5.11}$$

$$-P_l \leqslant p_{lt} \leqslant P_l,\ \ \forall l \in \mathbf{L}, t \in [1, T] \tag{5.12}$$

$$-\overline{\delta} \leqslant \delta_{nt} \leqslant \overline{\delta},\ \ \forall n \in \mathbf{N}, t \in [1, T] \tag{5.13}$$

$$0 \leqslant d_{nt} \leqslant q_{nt},\ \forall n \in \mathbf{N}, t \in [1, T] \tag{5.14}$$

where, $\mathbf{q} \in \mathbb{Q}$ is the uncertainty set defined in (5.15), which is similar to [55], to capture the uncertainty of demand.

$$\mathbb{Q}(\mathbf{q}, \mathbf{z}, \mathbf{k}) = \Big\{ q_{nt} \in [\underline{q}^{nt}, \underline{q}^{nt} + z_{nt} \triangle q^{nt}], \quad \sum_n z_{nt} \leqslant k_t, z_{nt} = \{0, 1\} \Big\}. \tag{5.15}$$

To be specific, constraints (5.2) and (5.3) are introduced to consider the startup costs as a monotone increasing step function of the unit's previous offline time (details can be found in [58]). Constraints (5.4) and (5.5) are the minimum up/down time constraints. (5.6) reflect the logic relationships between generator on-off status, turn-on and turn-off variables. Constraints (5.7) and (5.8) are ramping up/down constraints. Constraints(5.9) specify generator's active power level. Constraints(5.10) represent the Kirchhoff's law. Constraints (5.11) make sure the load is balanced at each bus. Constraints (5.12) specify the

active power flow limits on transmission lines. Constraints (5.13) are the phase angle limit. Constraints (5.14) guarantee the load shed on buses does not exceed their demand.

To simplify the notations in this chapter, we use the abstract form of the above formulation. Let $\mathbf{x}$ be the vector of all binary commitment variables and $\mathbf{U} = \{\mathbf{x} : \mathbf{Fx} \geqslant \mathbf{f}\}$ denote the associated feasible set defined by constraints in (5.2) - (5.6). Similarly, let $(\mathbf{y}, \mathbf{p})$ be the vector of continuous variables where $\mathbf{y}$ represents all generation level variables g_{jt} and $\mathbf{p}$ denote the rest of economic dispatch and market decision variables. Let $\mathbf{\Omega}(\mathbf{x}, \mathbf{q}) = \{(\mathbf{y}, \mathbf{p}) : \mathbf{Ax} + \mathbf{By} \leqslant \mathbf{g}, \mathbf{Cy} + \mathbf{Dp} + \mathbf{Eq} \leqslant \mathbf{h}, \mathbf{Gp} \geqslant \mathbf{r}\}$ be the associated feasible set defined by constraints in (5.7) - (5.14) for given $(\mathbf{x}, \mathbf{q})$. As a result, our RUC problem can be compactly represented as the following.

$$\min_{\mathbf{x} \in \mathbf{U}} \mathbf{ax} + \max_{\mathbf{q} \in \mathbb{Q}} \min_{(\mathbf{y}, \mathbf{p}) \in \mathbf{\Omega}(\mathbf{x}, \mathbf{q})} (\mathbf{by} + \mathbf{cp}) \tag{5.16}$$

5.3 Basic CCG Implementation for RUC

For the presented tri-level RUC problem, we use CCG method that iteratively computes RUC master problem and RUC subproblem. Note that RUC master problem is formulated with a subset of the worst-case demand scenarios, while RUC subproblem is a bi-level program which seeks for the worst-case scenario for a given commitment plan $\hat{\mathbf{x}}$.

5.3.1 RUC Master Problem

It is a relaxation of the original tri-level program with a subset of worst-case demand scenarios $\{\hat{\mathbf{q}}^s, s = 1, 2, ..., S\}$ generated by the RUC subproblem ($\hat{*}$ denotes a fixed decision variable or vector of $*$). The dispatch variables and constraints associated with each

scenario are included in the formulation. The solution of RUC master problem gives a commitment plan that is feasible with respect to the already included worst-case demand scenarios. Meanwhile, its optimal value gives a lower bound for the original RUC.

$$\min \beta + \mathbf{ax} \tag{5.17}$$

$$s.t.\ \mathbf{x} \in \mathbf{U} \tag{5.18}$$

$$\beta \geqslant \mathbf{by}^s + \mathbf{cp}^s, \quad s = 1, 2, ..., S \tag{5.19}$$

$$(\mathbf{y}^s, \mathbf{p}^s) \in \mathbf{\Omega}(\mathbf{x}, \hat{\mathbf{q}}^s),\ s = 1, 2, ..., S \tag{5.20}$$

where $\{(\mathbf{y}^s, \mathbf{p}^s)\}$ are the generation and dispatch decision variables for scenario s. Since RUC master problem is a single level MIP, it can be readily solved by most MIP solvers.

5.3.2 RUC Subproblem

For a given commitment plan $\hat{\mathbf{x}} = (\hat{u}_{jt}, \hat{v}_{jt}, \hat{w}_{jt})$ for the next T periods, we compute the following RUC subproblem to derive its optimal solution $(\hat{\mathbf{q}}^s, \hat{\mathbf{y}}^s, \hat{\mathbf{p}}^s)$. Note that (1). $\hat{\mathbf{q}}^s$ is a worst-case demand scenario with respect to $\hat{\mathbf{x}}$, which will be used to augment RUC master problem. (2). $(\hat{\mathbf{x}}, \hat{\mathbf{y}}^s, \hat{\mathbf{p}}^s)$ is a feasible solution to the overall RUC problem, which provides an upper bound.

$$\max_{\mathbf{q} \in \mathbb{Q}} \min(\mathbf{by} + \mathbf{cp}) \tag{5.21}$$

$$s.t.\ (\mathbf{y}, \mathbf{p}) \in \Omega(\hat{\mathbf{x}}, \mathbf{q}). \tag{5.22}$$

To solve such bi-level problem, strong duality or Karush-Kuhn-Tucker (KKT) conditions [17] can be employed to convert it into a single level nonlinear problem, which can then be linearized as an MIP and computed by solvers. Hence, the whole CCG procedure can simply be implemented with the help of an MIP solver.

5.3.3 Basic CCG Decomposition Framework

A basic implementation of the decomposition algorithm framework based on the column-and-constraint generation is described in Algorithm 4.

Algorithm 4 : Basic CCG algorithm for RUC

initialization:$ub \leftarrow \infty, lb \leftarrow -\infty, gap \leftarrow 1, s \leftarrow 0$
while $gap \geqslant \epsilon$ **do** ▷ ϵ is the predefined tolerable gap
    solve RUC master problem, update $lb, \hat{\mathbf{x}}, gap$
    solve RUC subproblem, update $ub, \hat{\mathbf{q}}^s, gap$
    add $\mathbf{\Omega}(\mathbf{x}, \hat{\mathbf{q}}^s)$ to RUC master problem
    $s = s + 1$
end while
return $\hat{\mathbf{x}}$ ■

5.4 RUC Master Problem Improvements

As mentioned in Section I, the computational performance of the basic CCG method might not be satisfactory to support real operations in large grids. In particular, we first note that more and more variables and constraints are created and included in RUC master problem over iterations, which lead to large-scale MIPs. We also observed that computing RUC subproblem is extremely time-consuming for large grids with full transmission network constraints. So, we study new computational methods and strategies to address such computational challenge, including incorporating strong formulations for basic UC model, deriving new valid inequalities considering network constraints for each worst-case scenario,

and designing and implementing a new decomposition procedure for computing robust unit commitment subproblem.

5.4.1 Strong Formulation for RUC Master Problem

The strong formulation is implemented as a technique to speed up the solution of deterministic UC [58, 59]. In [59], a set of tight constraints for the minimum up/down, and ramping up/down constraints is introduced, which has a clear positive impact on reducing computation time. So, we adopt those constraints in order to strengthen our RUC master problem since minimum up/down, and ramping up/down constraints are considered in the RUC master problem. Note that the strong formulation is used for each set of dispatch variables and constraints $\{(\mathbf{y}^s, \mathbf{p}^s)\} \in \mathbf{\Omega}(\mathbf{x}, \hat{\mathbf{q}}^s)$. For simplicity, we omit the demand scenario index s and generator index j in the following constraints.

For generation upper bound, constraints (5.23) serve to make the upper bound on power output a function of u_t, v_t and w_t.

$$g_t \leqslant \overline{G} u_{(t+K_t)} + \sum_{i=1}^{K_t} \{(SD + (i-1)RD) w_{t+i} - \overline{G} v_{t+i}\}, \forall t \in [1, T] \tag{5.23}$$

where $K_t = \max\{k \in \{1, ...UT\} | SD + (k-1)RD < \overline{G}, k + t < T\}$. This mean that if the generator is turned off at time $t+1$, then it cannot produce more than SD_j in t. If it is turned off in $t+2$, then it cannot produce more than $SD_j + RD_j$. Detailed explanations can be found in [59]. In our study, (5.23) are used instead of traditional generator upper bound constraints to provide a tighter linear program approximation to the original mixed-integer program based master problem.

Similarly, ramping down constraints (5.8) can be strengthened as (5.24), (5.25), and (5.26). If $RD > (SU - \underline{G})$ and $UT \geqslant 2$,

$$g_{t-1} - g_t \leqslant RDu_t + SDw_t - (RD - SU + \underline{G})v_{t-1} - (RD + \underline{G})v_t, \ \forall t \in [1, T]$$

$$\text{else, } g_{t-1} - g_{jt} \leqslant RDu_t + SDw_t, \qquad \forall t \in [1, T]. \tag{5.24}$$

If $RD > (SU - \underline{G})$, $UT \geqslant 3$, and $DT \geqslant 2$,

$$g_{t-1} - g_t \leqslant RDu_{t+1} + SDw_t + RDw_{t+1} - (RD + \underline{G})v_t$$

$$-(RD - SU + \underline{G})v_{t-1} - RDv_{t+1}, \ \ \forall t \in [1, T-1]. \tag{5.25}$$

(5.24) are valid inequalities and dominate (5.8). Constraints (5.25) take into account information from time $t + 1$ and constraints (5.26) consider ramping over two time periods.

$$g_{t-2} - g_t \leqslant 2RDu_t + SDw_{t-1} + (SD + RD_j)w_t - 2RDv_{t-2} - (2RD + \underline{G})v_{t-1}$$

$$-(2RD + \underline{G})v_t, \ \forall t \in [2, T-2]. \tag{5.26}$$

Ramping up constraints (5.27) and (5.28) are formulated to replace constraints (5.7) for each scenario in RUC master problem. If $RU > (SD - \underline{G})$ and $UT \geqslant 2$,

$$g_t - g_{t-1} \leqslant RUu_t - \underline{G}w_t - (RD - SU + \underline{G})w_{t+1} + (SU - RU)v_t, \ \ \forall t \in [1, T-1]$$

$$\text{else, } g_t - g_{t-1} \leqslant RUu_{t-1} + SUv_t, \ \forall t \in [1, T]. \tag{5.27}$$

If $RU > (SD - \underline{G})$, $UT \geqslant 2$, and $DT \geqslant 2$,

$$g_t - g_{t-2} \leqslant 2RUu_t - \underline{G}(w_{t-1} - w_t) + (SU - RU)v_{t-1} + (SU - 2RU)v_t, \forall t \in [2, T]. \quad (5.28)$$

The above tight constraints are used in the RUC master formulation to replace the classical minimum up/down and ramping up/down constraints.

5.5 Reformulation and Decomposition Algorithm for RUC Subproblem

As previously mentioned, for bi-level RUC subproblem, a traditional way is to convert it into a single level program by strong duality or KKT conditions. However, this process yields a huge MIP, which actually has a very weak linear program relaxation that is very difficult to compute for larger networks. To address such challenge, we novelly reformulate that bi-level program into a tri-level program by separating $\mathbf{y}$ and $\mathbf{p}$ variables. Specifically, we equivalently reformulate (5.21)-(5.22) as

$$\max_{\mathbf{q} \in \mathbb{Q}} \min(\mathbf{by} + \min \mathbf{cp}) \quad (5.29)$$

$$s.t.\ (\mathbf{y}, \mathbf{p}) \in \mathbf{\Omega}(\hat{\mathbf{x}}, \mathbf{q}). \quad (5.30)$$

Physically, such disconnection separates the generation level (defined by ramping constraints) decisions and dispatch decisions. Moreover, by dualizing the inner-most minimization problem, which computes the dispatching decisions for each individual hour, we have,

$$\max_{\mathbf{q} \in \mathbb{Q}} \min \left(\mathbf{by} + \max(\mathbf{y^T C^T} + \mathbf{q}^T \mathbf{E}^T - \mathbf{h}^T + \mathbf{r}^T)\boldsymbol{\pi} \right) \quad (5.31)$$

$$st.\ \mathbf{A}\hat{\mathbf{x}} + \mathbf{B}\mathbf{y} \leqslant \mathbf{g}, \tag{5.32}$$

$$(\mathbf{G}^T - \mathbf{D}^T)\boldsymbol{\pi} \leqslant \mathbf{c}^T. \tag{5.33}$$

Note, $(*)^T$ is the transpose of $(*)$ and $\boldsymbol{\pi}$ is the vector of dual variables. Again, we employ CCG method to decompose this tri-level formulation. To simplify our exposition, we call the master problem of this CCG implementation as "scenario master" and the subproblem as "scenario subproblem", which indicate that they are designed to solve RUC subproblem to derive the worst-case scenario.

5.5.1 Scenario Master Problem

The scenario master problem computes the worst-case demand scenario, for a set of feasible generation decisions $\{\hat{\mathbf{y}}^k, k = 1, ..., K\}$ (solutions from scenario subproblem).

$$\max \eta \tag{5.34}$$

$$s.t.\ \eta \leqslant \mathbf{b}\hat{\mathbf{y}}^k + (\hat{\mathbf{y}}^{kT}\mathbf{C}^T - \mathbf{h}^T + \mathbf{r}^T)\boldsymbol{\pi}^k \tag{5.35}$$

$$\mathbf{q} \in \mathbb{Q}, \tag{5.36}$$

$$\mathbf{A}\hat{\mathbf{x}} + \mathbf{B}\hat{\mathbf{y}}^k \leqslant \mathbf{g}, \tag{5.37}$$

$$(\mathbf{G}^T - \mathbf{D}^T)\boldsymbol{\pi}^k \leqslant \mathbf{c}^T, k = 1, ..., K. \tag{5.38}$$

Nonlinear constraints can be linearized and the whole formulation can be converted into an MIP.

5.5.2 Scenario Subproblem

The scenario subproblem is a DC economic dispatch problem with commitment plan $\hat{\mathbf{x}}$ given from the NCCG master problem and load scenario $\hat{\mathbf{q}}$ derived from the scenario master problem. The variables left in the scenario subproblem is the generating levels of generators, phase angles of buses, branch power flow, and the load shed. As a matter of fact, this subproblem is a linear program and only continuous variables are involved.

$$\min(\mathbf{by} + \mathbf{cp}) \tag{5.39}$$

$$s.t.\ (\mathbf{y}, \mathbf{p}) \in \mathbf{\Omega}(\hat{\mathbf{x}}, \hat{\mathbf{q}}). \tag{5.40}$$

5.6 Improved Algorithm Framework

Combining the above improvements, the new algorithm can be stated as in Algorithm 5 where the subroutine matches the reformulation and decomposition algorithm for bi-level RUC subproblem.

5.7 Computational Results

The computational study is conducted on a dual-core PC with 4GB RAM. The CPLEX 12.6 is used to solve the MIP or linear program. The program is implemented with C++ and Visual Studio. The IEEE 118-bus system with 54 generators and 186 transmission lines is used as a test system.

First of all, we compare the effectiveness of the reformulation and decomposition for RUC subproblem with traditional strong duality based approach (used in [50, 57]) in Table 18. Four random instances are tested. The exit condition is either optimal (denoted by O)

Algorithm 5 : Improved CCG algorithm for RUC

procedure (CCG)
  initialization:$ub \leftarrow \infty, lb \leftarrow -\infty, gap \leftarrow 1, s \leftarrow 0$
  while $gap \geqslant \epsilon$ **do**
    solve RUC master problem with strong formulation and constraints (**??**), update $lb, \hat{\mathbf{x}}, gap$
    solve RUC bi-level subproblem through **Subroutine**, update $ub, \hat{\mathbf{q}}^s, gap$
    add $\mathbf{\Omega}(\mathbf{x}, \hat{\mathbf{q}}^s)$ to RUC master problem
    $s = s + 1$
  end while
  return $\hat{\mathbf{x}}$ ■
end procedure

Subroutine: Solving RUC subproblem

procedure (RUC subproblem)
  initialization:$ub^{'} \leftarrow \infty, lb^{'} \leftarrow -\infty, gap^{'} \leftarrow 1, k \leftarrow 0$
  while $gap^{'} \geqslant \epsilon^{'}$ **do**
    solve scenario master problem, update $ub^{'}, gap^{'}$
    solve scenario subproblem, update $lb^{'}, \hat{\mathbf{y}}^k, gap^{'}$
    add $\{\boldsymbol{\pi}^k, \hat{\mathbf{y}}^k$,(5.37-5.38)$\}$ to scenario master problem
    $k = k + 1$
  end while
  return $\hat{\mathbf{q}}$
end procedure

where the gap is within 0.1% or computational time reaches 10 minutes time limit (denoted by T). Using the traditional strong duality-based single level reformulation approach, all instances stopped after reaching the time limit. By using the CCG reformulation, all instances reached optimal solutions within the time limit. It clearly shows that the improved decomposition algorithm is much more effective. To further test our improved algorithm, a comparison between Algorithms 2 and the basic CCG method, i.e., Algorithm 1 with strong duality, is given in Table 19. The exit condition is the optimal gap with 1% (O) or the time limit of 100 minutes (T). As can be seen in Table 19, the basic CCG cannot solve any of the instances to optimality within the 100-minute time limit. However, our improved algo-

Table 18: Computational results for RUC subproblem

case ID	strong duality		CCG reformulation	
	exit	gap	exit	time (s)
1	T	1.24%	O	28.5 (2 iterations)
2	T	2.01%	O	29.9 (2 iterations)
3	T	2.98%	O	226.5(3 iterations)
4	T	3.31%	O	312.5(3 iterations)

Table 19: Computational results for robust unit commitment

case ID	Algorithm 4 + strong duality		Algorithm 5	
	exit	gap	exit	time (s)
1	T	3.10%	O	164
2	T	2.79%	O	550
3	T	4.20%	O	1325
4	T	4.41%	O	3228

rithm can solve all the instances to optimality within the time limit. Generally, we observe the improved algorithm performs much faster than the basic CCG method and can handle cases that basic method cannot solve in a reasonably long time. Therefore, it significantly improves our computing capability to handle large-size power grids.

5.8 Conclusion

In this chapter, we developed a new fast computing method for the two-stage robust unit commitment problem. Strong formulation and network based valid inequalities are developed to speed up the RUC master problem solution process. For the RUC subproblem, which is a bi-level program, a novel tri-level reformulation and decomposition strategy is designed, which actually dramatically decreases the computational complexity of solving the bi-level program through strong duality based reformulation. The improved algorithm performs significantly faster than the basic CCG method.

CHAPTER 6: CONCLUDING REMARKS

This dissertation addresses the issue of uncertainties from terrorist attacks, natural disasters and uncertain demand in the power system operation and planning problems through a defender-attack-defender game theoretic model or two-stage robust optimization. Decomposition algorithms are provided, customized and improved to solve each individual problem.

Chapter 2 and Chapter 3 describe a power system transmission network protection or hardening planning problem, which is formulated as a defender-attack-defender sequential game. In Chapter 2, an exact solution is given to the traditional power grid defender-attack-defender model. The effectiveness of protection is validated through computational studies. In Chapter 3, network topology control through transmission switching is introduced to the defender-attacker-defender model as a corrective approach to alleviate system damage under attack. A nested decomposition algorithm is designed and implement to solve this model. Cost-effectiveness of network topology control is validated. Chapter 4 proposes a decision support tool for the planning of a resilient distribution network against uncertain natural disasters using hardening and distributed generation resources. Chapter 5 presents a fast computing method for the two-stage robust unit commitment problem.

REFERENCES

[1] W. Yuan, L. Zhao, and B. Zeng, "Optimal power grid protection through a defender-attacker-defender model," *Reliability Engineering & System Safety*, vol. 121, pp. 83–89, 2014.

[2] Committee on Enhancing the Robustness and Resilience of Future Electrical Transmission and Distribution in the United States to Terrorist Attack; Board on Energy and Environmental Systems; National Research Council, *Terrorism and the Electric Power Delivery System*. The National Academies Press, 2012.

[3] R. Zimmerman, C. Restrepo, J. Simonoff, and L. Lave, "Risk and economic costs of a terrorist attack on the electric system," *The Economic Costs and Consequences of Terrorism*, p. 273, 2008.

[4] J. Glover, M. Sarma, and T. Overbye, *Power System Analysis and Design: Fifth Edition*. Thomson Engineering, 2011.

[5] A. Delgadillo, J. Arroyo, and N. Alguacil, "Analysis of electric grid interdiction with line switching," *Power Systems, IEEE Transactions on*, vol. 25, no. 2, pp. 633–641, 2010.

[6] A. Wood and B. Wollenberg, *Power generation, operation, and control*. Wiley New York, 1996, vol. 2.

[7] J. Salmeron, K. Wood, and R. Baldick, "Analysis of electric grid security under terrorist threat," *Power Systems, IEEE Transactions on*, vol. 19, no. 2, pp. 905–912, 2004.

[8] ——, "Worst-case interdiction analysis of large-scale electric power grids," *Power Systems, IEEE Transactions on*, vol. 24, no. 1, pp. 96–104, 2009.

[9] A. Motto, J. Arroyo, and F. Galiana, "A mixed-integer lp procedure for the analysis of electric grid security under disruptive threat," *Power Systems, IEEE Transactions on*, vol. 20, no. 3, pp. 1357–1365, 2005.

[10] L. Zhao and B. Zeng, "Vulnerability analysis of power grids with line switching," *Power Systems, IEEE Transactions on*, vol. 28, no. 3, pp. 2727–2736, 2013.

[11] G. Brown, M. Carlyle, J. Salmeron, and K. Wood, "Defending critical infrastructure," *Interfaces*, vol. 36, no. 6, pp. 530–544, 2006.

[12] Y. Yao, T. Edmunds, D. Papageorgiou, and R. Alvarez, "Trilevel optimization in power network defense," *Systems, Man, and Cybernetics, Part C: Applications and Reviews, IEEE Transactions on*, vol. 37, no. 4, pp. 712–718, july 2007.

[13] G. Brown, M. Carlyle, J. Salmeron, and K. Wood, "Analyzing the vulnerability of critical infrastructure to attack and planning defenses," in *Tutorials in Operations Research. INFORMS*. INFORMS, 2005, pp. 102–123.

[14] V. Bier, E. Gratz, N. Haphuriwat, W. Magua, and K. Wierzbicki, "Methodology for identifying near-optimal interdiction strategies for a power transmission system," *Reliability Engineering & System Safety*, vol. 92, no. 9, pp. 1155–1161, 2007.

[15] A. Delgadillo, J. Arroyo, and N. Alguacil, "Power system defense planning against multiple contingencies," in *17th Power Systems Computation Conference (PSCC11), Stockholm*, 2011.

[16] E. Israeli, "System interdiction and defense." DTIC Document, Tech. Rep., 1999.

[17] B. Zeng and L. Zhao, "Solving two-stage robust optimization problems using a column-and-constraint generation method," *Operations Research Letters*, vol. 41, no. 5, pp. 457–461, september 2013.

[18] C. Grigg, P. Wong, P. Albrecht, R. Allan, M. Bhavaraju, R. Billinton, Q. Chen, C. Fong, S. Haddad, S. Kuruganty, W. Li, R. Mukerji, D. Patton, N. Rau, D. Reppen, A. Schneider, M. Shahidehpour, and C. Singh, "The IEEE reliability test system–1996," *Power Systems, IEEE Transactions on*, vol. 14, no. 3, pp. 1010–1020, 1999.

[19] Executive office of the President, White House, Washington, "Economic benefits of increasing electric grid resilience to weather outages," August 2013.

[20] Committee on Science and Technology for Countering Terrorism, National Research Council, *Making the Nation Safer:The Role of Science and Technology in Countering Terrorism*. The National Academies Press, 2002.

[21] M. G. Frodl and J. M. Manoyan, "Energy security starts with hardening power grids," *National Defense-Journal of the American Defense Preparedness Association*, vol. 97, no. 708, 2012.

[22] N. Alguacil, A. Delgadillo, and J. Arroyo, "A trilevel programming approach for electric grid defense planning," *Computers & Operations Research*, vol. 41, no. 0, pp. 282 – 290, 2014.

[23] H. Glavitsch, "Switching as means of control in the power system; state of the art review," *Electrical Power & Energy Systems*, vol. 7, no. 2, 1985.

[24] W. Shao and V. Vittal, "Corrective switching algorithm for relieving overloads and voltage violations," *Power Systems, IEEE Transactions on*, vol. 20, no. 4, pp. 1877–1885, 2005.

[25] M. Golari, N. Fan, and J. Wang, "Two-stage stochastic optimal islanding operations under severe multiple contingencies in power grids," *Electric Power Systems Research*, vol. 114, pp. 68–77, 2014.

[26] R. L.-Y. Chen, N. Fan, A. Pinar, and J.-P. Watson, "Contingency-constrained unit commitment with post-contingency corrective recourse," *Annals of Operations Research*, pp. 1–27, 2014.

[27] K. Hedman, S. Oren, and R. O'Neill, "A review of transmission switching and network topology optimization," in *Power and Energy Society General Meeting, 2011 IEEE*. IEEE, 2011, pp. 1–7.

[28] E. Fisher, R. O'Neill, and M. Ferris, "Optimal transmission switching," *Power Systems, IEEE Transactions on*, vol. 23, no. 3, pp. 1346–1355, 2008.

[29] F. Qiu and J. Wang, "Chance-constrained transmission switching with guaranteed wind power utilization," *Power Systems, IEEE Transactions on*, vol. PP, no. 99, pp. 1–9, 2014.

[30] J. Arroyo and F. Fernandez, "A genetic algorithm approach for the analysis of electric grid interdiction with line switching," in *Intelligent System Applications to Power Systems, 2009, 15th International Conference on*. IEEE, 2009, pp. 1–6.

[31] L. Zhao and B. Zeng, "An exact algorithm for two-stage robust optimization with mixed integer recourse problems," Technical Report, University of South Florida, available in *optimization-online*, 2012.

[32] J. Arroyo, "Bilevel programming applied to power system vulnerability analysis under multiple contingencies," *Generation, Transmission & Distribution, IET*, vol. 4, pp. 178–190, 2010.

[33] United States Government Accountability Office, "Climate change: Energy infrastructure risks and adaptation efforts," January 2014.

[34] W. Yuan and B. Zeng, "Achieving cost-effective power grid hardening through transmission network topology control," under review, available in *optimization-online*, 2014.

[35] M. E. Baran and F. F. Wu, "Network reconfiguration in distribution systems for loss reduction and load balancing," *Power Delivery, IEEE Transactions on*, vol. 4, no. 2, pp. 1401–1407, 1989.

[36] E. Yamangil, R. Bent, and S. Backhaus, "Designing resilient electrical distribution grids," *arXiv preprint arXiv*, 2014.

[37] C. Lee, C. Liu, S. Mehrotra, and Z. Bie, "Robust distribution network reconfiguration," *Smart Grid, IEEE Transactions on*, vol. 6, no. 2, pp. 836–842, 2015.

[38] C. Chen, J. Wang, F. Qiu, and D. Zhao, "Resilient distribution system by microgrids formation after natural disasters," *Smart Grid, IEEE Transactions on*, in press, 2015.

[39] C. L. Borges and D. M. Falcao, "Optimal distributed generation allocation for reliability, losses, and voltage improvement," *International Journal of Electrical Power & Energy Systems*, vol. 28, no. 6, pp. 413–420, 2006.

[40] P. S. Georgilakis and N. D. Hatziargyriou, "Optimal distributed generation placement in power distribution networks: Models, methods, and future research," *IEEE Trans. Power Syst*, vol. 28, no. 3, pp. 3420–3428, 2013.

[41] Z. Wang, B. Chen, J. Wang, J. Kim, and M. M. Begovic, "Robust optimization based optimal DG placement in microgrids," *Smart Grid, IEEE Transactions on*, vol. 5, no. 5, pp. 2173–2182, 2014.

[42] N. Alguacil, A. Delgadillo, and J. M. Arroyo, "A trilevel programming approach for electric grid defense planning," *Computers & Operations Research*, vol. 41, pp. 282–290, 2014.

[43] T. T. H. Pham, Y. Bésanger, and N. Hadjsaid, "New challenges in power system restoration with large scale of dispersed generation insertion," *Power Systems, IEEE Transactions on*, vol. 24, no. 1, pp. 398–406, 2009.

[44] Y. Wang, C. Chen, J. Wang, and R. Baldick, "Research on resilience of power systems under natural disasters - a review," *Power Systems, IEEE Transactions on*, in press, 2015.

[45] N. H. Center. Hurricane decay: Demise of a hurricane. [Online]. Available: http://www.hurricanescience.org/science/science/hurricanedecay/

[46] J. Kaplan and M. DeMaria, "A simple empirical model for predicting the decay of tropical cyclone winds after landfall," *Journal of applied meteorology*, vol. 34, no. 11, pp. 2499–2512, 1995.

[47] D. Bertsimas, E. Litvinov, X. A. Sun, J. Zhao, and T. Zheng, "Adaptive robust optimization for the security constrained unit commitment problem," *Power Systems, IEEE Transactions on*, vol. 28, no. 1, pp. 52–63, 2013.

[48] C. Lee, C. Liu, S. Mehrotra, and M. Shahidehpour, "Modeling transmission line constraints in two-stage robust unit commitment problem," *Power Systems, IEEE Transactions on*, vol. 29, no. 3, pp. 1221–1231, 2014.

[49] C. Ruiz and A. Conejo, "Robust transmission expansion planning," *European Journal of Operational Research*, vol. 242, no. 2, pp. 390–401, 2015.

[50] L. Zhao and B. Zeng, "Robust unit commitment problem with demand response and wind energy," in *Power and Energy Society General Meeting, 2012 IEEE*. IEEE, 2012, pp. 1–8.

[51] R. M. Lima, A. Q. Novais, and A. J. Conejo, "Weekly self-scheduling, forward contracting, and pool involvement for an electricity producer. an adaptive robust optimization approach," *European Journal of Operational Research*, vol. 240, no. 2, pp. 457–475, 2015.

[52] A. Street, F. Oliveira, and J. M. Arroyo, "Contingency-constrained unit commitment with security criterion: A robust optimization approach," *Power Systems, IEEE Transactions on*, vol. 26, no. 3, pp. 1581–1590, 2011.

[53] S. Tan, J.-X. Xu, and S. K. Panda, "Optimization of distribution network incorporating distributed generators: an integrated approach," *Power Systems, IEEE Transactions on*, vol. 28, no. 3, pp. 2421–2432, 2013.

[54] X. Guan, P. Luh, H. Yan, and J. Amalfi, "An optimization-based method for unit commitment," *International Journal of Electrical Power & Energy Systems*, vol. 14, no. 1, pp. 9–17, 1992.

[55] D. Bertsimas, E. Litvinov, X. A. Sun, J. Zhao, and T. Zheng, "Adaptive robust optimization for the security constrained unit commitment problem," *IEEE Trans. Power Syst.*, vol. 28, no. 1, pp. 52–63, 2013.

[56] R. Jiang, J. Wang, and Y. Guan, "Robust unit commitment with wind power and pumped storage hydro," *IEEE Trans. Power Syst.*, vol. 27, no. 2, pp. 800–810, 2012.

[57] R. Jiang, M. Zhang, G. Li, and Y. Guan, "Benders decomposition for the two-stage security constrained robust unit commitment problem," Technical Report, available in *optimization-online*, 2011.

[58] G. Morales-Espana, J. Latorre, and A. Ramos, "Tight and compact milp formulation for the thermal unit commitment problem," *IEEE Trans. Power Syst.*, vol. 28, no. 4, pp. 4897–4908, 2013.

[59] J. Ostrowski, M. F. Anjos, and A. Vannelli, "Tight mixed integer linear programming formulations for the unit commitment problem," *Power Systems, IEEE Transactions on*, vol. 27, no. 1, pp. 39–46, 2012.

APPENDICES

Appendix A Copyright Permissions

A.1 Permission to Reuse Reference [1] for Chapter 2